



## OPEN Aniracetam restores the excitation-inhibition balance of neurotransmitters in the prefrontal cortex of mice with ADHD

Jie Cui<sup>1,2</sup>, Xiao-Li Sun<sup>3</sup>, Shuo Shi<sup>1,2</sup>, Hui Bai<sup>4</sup>, Wei Zhang<sup>5</sup>✉ & Wan-Jun Bai<sup>2</sup>✉

Attention-deficit/hyperactivity disorder (ADHD) is the most prevalent neurodevelopmental disorder in childhood and a common chronic condition among school-aged children. However, the pharmacological mechanisms and pathophysiology of ADHD remain incompletely elucidated. Transmembrane  $\alpha$ -amino-3-hydroxy-5-methyl-4-isoxazolepropionic acid (AMPA) receptor regulatory protein  $\gamma$ -8 (TARP  $\gamma$ -8, also known as calcium voltage-gated channel auxiliary subunit  $\gamma$ 8) functions as an auxiliary subunit of AMPA receptors. Previous studies suggest that mice lacking the TARP  $\gamma$ -8 protein may display hyperactivity, impulsivity, and memory deficits, which are hallmarks of ADHD. The nootropic compound aniracetam effectively mitigates ADHD-like symptoms, including hyperactivity, impulsivity, anxiety, cognitive deficits, and memory impairment, observed in adolescent TARP  $\gamma$ -8 knockout (KO) mice. This investigation explored the therapeutic potential of aniracetam and its underlying molecular mechanisms using TARP  $\gamma$ -8 KO mice as an ADHD model. Through cerebral microdialysis coupled with liquid chromatography-tandem mass spectrometry (UPLC-MS/MS) analysis, we identified perturbations in neurotransmitter metabolism in the ADHD model of TARP  $\gamma$ -8 KO mice. Real-time quantitative PCR (RT-qPCR) was employed to detect alterations in the expression of key receptor and transporter genes. The results indicate that aniracetam can alleviate ADHD-related behavioral deficits by modulating the excitatory-inhibitory neurotransmitter systems through the modulation of glutamate receptor,  $\gamma$ -Aminobutyric Acid receptor, and monoamine neurotransmitter transporter expression. These findings in a TARP  $\gamma$ -8-deficient ADHD model support further investigation into aniracetam as a potential therapeutic intervention for ADHD, providing novel molecular targets and a theoretical framework for the pharmacological management of ADHD.

**Keywords** Aniracetam, Attention deficit hyperactivity disorder, AMPA receptor, TARP  $\gamma$ -8, Neurotransmitters, Prefrontal cortex

According to the diagnostic and statistical manual of mental disorders, fifth edition (DSM-5), hyperactivity, inattention, impulsive behavior, and difficulties with social and academic functioning are the hallmarks of Attention-Deficit/Hyperactivity condition (ADHD), a neurodevelopmental condition. Between the ages of 6 and 17, ADHD most often manifests itself in youngsters, with a prevalence ranging from 3.4 to 7.2%<sup>1–3</sup>. Moreover, research indicates that 60 to 80% of cases persist into adulthood<sup>4</sup>. The disease can have a significant impact on children's social interactions, mental health, and academic performance, placing a heavy strain on both individuals and society as a whole<sup>5–7</sup>.

Although the precise etiology and pathogenic mechanisms of ADHD are still not entirely understood, research suggests that the disorder is brought on by intricate interplay between environmental circumstances and genetic

<sup>1</sup>Graduate School of Hebei Medical University, Shijiazhuang 050017, Hebei, China. <sup>2</sup>Department of Pharmacy, Hebei Key Laboratory of Clinical Pharmacy, Hebei General Hospital, NO. 348 West Heping Road, Shijiazhuang 050051, Hebei, China. <sup>3</sup>Department of Pharmacy, Hebei Key Laboratory of Clinical Pharmacy, Fourth Hospital of Hebei Medical University, Shijiazhuang 050017, Hebei, China. <sup>4</sup>The Second Hospital of Hebei Medical University, Shijiazhuang 050000, Hebei, China. <sup>5</sup>Department of Pharmacology, The Key Laboratory of Neural and Vascular Biology, Ministry of Education, The Key Laboratory of New Drug Pharmacology and Toxicology, Institution of Chinese Integrative Medicine, Hebei Medical University, Shijiazhuang 050017, Hebei, China. ✉email: weizhang@hebm.u.edu.cn; baiwanjun0311@163.com

predispositions<sup>8</sup>. Neurotransmitters like dopamine (DA) and norepinephrine (NE) work together through a variety of receptors to collectively alter the activity of the prefrontal cortex (PFC), cerebellum, and caudate nucleus-areas of the brain that control attention, thought, emotion, behavior, and motor skills<sup>9,10</sup>. Research has indicated that the primary functional impairments seen in people with ADHD are specifically linked to these brain regions<sup>9</sup>. It has been reported that polymorphisms in the genes encoding the dopamine D4 receptor (DRD4), DA transporter 1 (DAT-1), and serotonin 1B receptor (5-HT1B) can lead to neurotransmission dysfunction<sup>11–13</sup>. Many studies have shown that several genes are closely linked to the pathogenesis of ADHD in children, and the genes that have been identified thus far have all been strongly linked to neurotransmitter transmission and neurodevelopment, which is important information for understanding the pathological mechanisms and etiology of ADHD. These genes are mainly involved in the dopaminergic, serotonergic, noradrenergic, cholinergic, glutamatergic, and GABAergic pathways, and they may interact with environmental factors<sup>14,15</sup>. It is interesting to note that some of the genes found in human studies have been confirmed in animal models, while others are still pending confirmation<sup>16</sup>.

These interactions between the catecholaminergic and glutamatergic systems have led to an increasing amount of research evidence in recent years that the glutamatergic system is also extensively involved in the pathogenesis and development of ADHD<sup>17</sup>. As the central excitatory neurotransmitter, glutamate's dysfunctional signaling contributes to numerous neurological pathologies<sup>18</sup>. One of the key receptor targets of glutamate (Glu)-the  $\alpha$ -amino-3-hydroxy-5-methyl-4-isoxazolepropionic acid (AMPA)-type ionotropic Glu receptor family-plays a critical role in neurobiological processes underlying learning and memory<sup>19,20</sup>. Research indicates that regulatory drugs targeting AMPA receptors (AMPA) can positively modulate these neural processes, including synaptic plasticity and long-term potentiation (LTP)<sup>21,22</sup>. Building on these positive benefits, AMPARs and their allosteric modulators have become important targets for treatment in a variety of cognitive diseases, such as ADHD<sup>23,24</sup>, Parkinson's disease<sup>25,26</sup>, Alzheimer's disease<sup>27,28</sup>, and schizophrenia<sup>29–31</sup>. While the DA/NE system and other mechanisms are also associated with ADHD, it is proposed that a dysregulation of the bidirectional dopaminergic-glutamatergic interplay constitutes a core pathophysiological mechanism for ADHD-related behavioral deficits<sup>32–34</sup>. An alternative theory suggests that the inhibition of context-inappropriate responses is hampered by malfunction in the Glu- $\gamma$ -aminobutyric acid (GABA) circuit<sup>35</sup>. Specifically, increased calcium ion permeability and decreased neuronal membrane resistance caused by elevated Glu levels can cause cortical hyperexcitability. Conversely, weakened GABAergic inhibition makes the excitation-inhibition (E/I) imbalance even worse<sup>36</sup>. GABA and Glu, the major inhibitory and excitatory neurotransmitters in the central nervous system (CNS), have attracted increasing attention in ADHD research. Studies have shown that the balance between Glu and GABA in the prefrontal-striatal circuit is critical for normal brain development and function<sup>37,38</sup>. GABA primarily exerts its effects through medium spiny neurons in the striatum and interneurons in the cortex<sup>39,40</sup>. Several lines of evidence suggest that GABA plays a role in the neurophysiological mechanisms of ADHD<sup>15,41–43</sup>. For example, studies using magnetic resonance spectroscopy (MRS) have shown that children with ADHD have lower prefrontal GABA levels<sup>44</sup>, while another study found that similar prefrontal regions had higher glutamatergic levels<sup>35</sup>. Transmembrane AMPARs regulatory protein  $\gamma$ -8 (TARP  $\gamma$ -8), a key protein regulating the basal expression, synaptic localization, and plasticity of AMPARs, has been closely linked to the development of ADHD. Notably, TARP  $\gamma$ -8 deficiency in adolescent mice leads to typical ADHD-like phenotypes, including hyperactivity, impulsivity, anxiety, and cognitive impairment, thereby recapitulating core symptoms and common comorbidities of the disorder<sup>45,46</sup>. Synaptosomal proteomic analysis revealed dysregulated dopaminergic and glutamatergic transmission in the PFC of adolescent TARP  $\gamma$ -8 knockout (KO) mice, alongside impaired AMPARs complex function in the hippocampus<sup>47,48</sup>. These findings indicate that adolescent TARP  $\gamma$ -8 KO mice may serve as a novel and etiologically relevant animal model for ADHD research<sup>49</sup>. Population studies further support the genetic underpinnings of TARP  $\gamma$ -8 in ADHD. Large-scale genome-wide analyses have identified significant associations between common single-nucleotide polymorphisms (e.g., rs11084307) within the *CACNG8* locus and an increased risk for ADHD, establishing it as a susceptibility gene<sup>50</sup>. Subsequent functional genomic studies further suggest that these risk-associated genetic variants may lead to downregulation of *CACNG8* gene expression or impairment of TARP  $\gamma$ -8 protein function, potentially affecting its fine-tuned regulation of excitatory synaptic signaling in key brain regions such as the hippocampus<sup>24,49,51</sup>. This finding from human genetics strongly aligns with the core ADHD-like behavioral phenotypes-including hyperactivity, impulsivity, and attention deficits-that are stably recapitulated in TARP  $\gamma$ -8 KO mouse models and are reversible with first-line treatments such as methylphenidate<sup>24,47,48</sup>. Therefore, integrating evidence from human genetic susceptibility and animal model phenotypes, *CACNG8* and its encoded TARP  $\gamma$ -8 protein are recognized as important genetic factors involved in the pathophysiology of ADHD<sup>52,53</sup>.

Aniracetam (1-[(4-methoxyphenyl)]-2-pyrrolidinone), a nootropic drug of the piracetam class, is characterized by its mild side effects<sup>54</sup>. Aniracetam exerts its effects through a dual allosteric modulation mechanism targeting both AMPARs and metabotropic Glu receptors (mGluRs). It not only directly enhances glutamatergic synaptic transmission but also activates neuronal nicotinic acetylcholine receptors (nAChRs), thereby indirectly promoting dopaminergic neurotransmission via cholinergic activity<sup>55</sup>. Aniracetam is known to postpone receptor desensitization and deactivation by maintaining the Glu-bound conformation of AMPARs, which in turn affects ion flux<sup>21,56,57</sup>. Aniracetam safely and successfully reduces emotional dysregulation, sleep problems, and cognitive impairment in people with Alzheimer's disease<sup>58,59</sup> and cerebrovascular illnesses, according to clinical research<sup>60–62</sup>. Animal studies have demonstrated that piracetam improves memory dysfunction following brain injury, reverses scopolamine-induced deficits in passive avoidance tasks, and provides neuroprotection against scopolamine or CO<sub>2</sub> intoxication<sup>63–65</sup>. It has been shown to improve cognitive function and ameliorate ADHD-like behaviors in TARP  $\gamma$ -8 KO mice<sup>49,66</sup>. However, a comprehensive understanding of its effects on the neurotransmitter networks underlying these behavioral improvements is lacking.

Therefore, microdialysis sampling combined with Ultra Performance Liquid Chromatography-Tandem Mass Spectrometry (UPLC-MS/MS) analysis was utilized to assess the regulatory effects of aniracetam-a positive allosteric modulator of AMPARs-on the neurotransmitter network in the PFC of TARP  $\gamma$ -8 KO mice. By quantitatively monitoring dynamic changes in the homeostasis of multiple neurotransmitter systems, including DA, serotonin (5-HT), 5-hydroxyindoleacetic acid (5-HIAA), Glu, Glycine (Gly), and GABA, and integrating Real-time quantitative PCR (RT-qPCR) to analyze mRNA expression profiles of key receptor subunits and transporters, this study provides deeper mechanistic insights into how aniracetam modulates the PFC neurotransmitter system under TARP  $\gamma$ -8 deficiency.

## Materials and methods

### Chemicals and reagents

Glutamate (Glu, Lot: B25300, purity  $\geq$  98%), Glycine (Gly, Lot: B21915, purity  $\geq$  99%),  $\gamma$ -aminobutyric acid (GABA, Lot: B21979, purity  $\geq$  99%), serotonin (5-HT, Lot: B21833, purity  $\geq$  98%), 5-hydroxyindoleacetic acid (5-HIAA, Lot: B27047, purity  $\geq$  98%), and dopamine (DA, Lot: B25300, purity  $\geq$  98%) were purchased from Shanghai Yuanye Bio-Technology Co., Ltd. Isoprenaline (ISO, Lot: I8480, purity  $\geq$  98%) was obtained from Solarbio. Aniracetam (Lot: T0333, purity  $\geq$  99.8%) and hydroxypropyl- $\beta$ -cyclodextrin (HP- $\beta$ -CD, Lot: T19609, purity  $\geq$  98%) were supplied by TargetMol. TRIzol<sup>®</sup> Reagent (Lot: 99940401) was acquired from Invitrogen (USA). The FastKing cDNA First Strand Synthesis Kit (Cat: KR118-01) and RealUniversal Color Fluorescence Quantitative PreMix Kit (Cat: FP201-02) were procured from Tiangen Biotech (Beijing) Co., Ltd. Purified water was provided by Hangzhou Wahaha Group Co., Ltd. Acetonitrile and methanol (both HPLC grade) were sourced from Thermo Fisher Scientific, and formic acid (HPLC grade) was supplied by Shandong Xiya Chemical Co., Ltd.

### Apparatus and software

The ultra-performance liquid chromatography (UPLC) system (LC-30A), equipped with a binary high-pressure gradient pump (LC-30AD), a column oven (CTO-30A), and an autosampler (SIL-30AC), was obtained from Shimadzu Corporation (Japan). The AB Sciex 5500 triple quadrupole mass spectrometer, featuring a Turbo V<sup>™</sup> electrospray ionization source and triple quadrupole mass analyzer, along with Analyst<sup>®</sup> 1.6.1 data acquisition software, was acquired from AB Sciex (USA). Additional equipment included: a NewClassic analytical balance (Mettler Toledo, Switzerland); pipettes (Eppendorf, Germany); a vortex mixer (Thermo Scientific); a KQ-5200E ultrasonic cleaner (Kunshan Ultrasonic Instrument Co., Ltd., China); an S1010E centrifuge (SCIOGEX, USA); a -80 °C ultra-low temperature freezer (Thermo Fisher Scientific, USA); and an intracerebral microdialysis system from BASi (USA), comprising MD-2211 probes (1 mm membrane length), MD-2255 guide cannulae, an MD-406 animal activity system, MW-2310 sampling needles, and an MD-1201 refrigerated auto-sampler. A Hamilton microsyringe, a stereotaxic instrument for mice, a handheld cranial drill, and a small animal anesthesia machine were purchased from RWD Life Science Co., Ltd. (Shenzhen, China).

### Animals and treatment

This study was approved by the Animal Ethics Committee of the General Hospital of Hebei (Approval No.: 2024-DW-038, Shijiazhuang, China). All experimental procedures were conducted in accordance with the ethical guidelines and regulations for animal welfare established by the General Hospital of Hebei and followed the recommendations of the ARRIVE guidelines for reporting in vivo experiments. The TARP  $\gamma$ -8 KO mouse strain used in the experiments had been backcrossed for at least eight generations onto a C57BL/6 J background. Homozygous TARP  $\gamma$ -8 KO mice and their wild-type (WT) littermate controls were obtained by crossing heterozygous parents. Animals were group-housed by genotype (6 mice per cage) under controlled environmental conditions: temperature was maintained at 22  $\pm$  0.5 °C, humidity at 50%  $\pm$  5%, and a 12 h light/dark cycle (lights on from 19:00 to 7:00) was applied. Food and water were available ad libitum. Male C57BL/6 J mice aged 4–8 weeks (body weight 13.2–20.5 g) were used and assigned to three groups based on genotype and treatment: WT (vehicle) group (WT, n = 8): Received intraperitoneal injection of a 10% HP- $\beta$ -CD aqueous solution at a volume of 10 mL/kg for 7 consecutive days. TARP  $\gamma$ -8 KO (vehicle) group (KO, n = 8): Received intraperitoneal injection of a 10% HP- $\beta$ -CD aqueous solution at a volume of 10 mL/kg for 7 consecutive days. TARP  $\gamma$ -8 (aniracetam) group (Aniracetam, n = 8): received intraperitoneal injection of a 10% HP- $\beta$ -CD inclusion complex solution containing aniracetam at a dose of 100 mg/kg for 7 consecutive days.

All drug solutions were freshly prepared immediately before administration. All mice were housed under identical conditions, and the drug administration procedures were kept consistent across all groups.

### Standard solution and quality control samples

Weighing six reference standards was done precisely. To create individual stock solutions at 1 mg·mL<sup>-1</sup>, Glu was dissolved in ultrapure water while the other neurotransmitter reference standards were dissolved in methanol. These solutions were then kept at -20 °C. A mixed standard solution was prepared in acetonitrile–water solution (4:1, v/v) with the following concentrations: 0.5  $\mu$ g·mL<sup>-1</sup> for Glu and DA, 0.3  $\mu$ g·mL<sup>-1</sup> for GABA and 5-HT, 10  $\mu$ g·mL<sup>-1</sup> for Gly, and 2  $\mu$ g·mL<sup>-1</sup> for 5-HIAA. The corresponding standard/quality control (QC) samples were prepared by serial dilution using artificial cerebrospinal fluid (aCSF) buffer. Additionally, 1 mg of the internal standard, isoprenaline hydrochloride, was accurately weighed and dissolved in methanol to obtain a 1 mg·mL<sup>-1</sup> stock solution, which was further diluted with acetonitrile–water (4:1, v/v) to a final concentration of 2 ng·mL<sup>-1</sup> and stored under refrigeration for subsequent use.

### aCSF

Weigh out the following: 101.65 mg of magnesium chloride hexahydrate ( $\text{MgCl}_2 \cdot 6\text{H}_2\text{O}$ ), 100.65 mg of potassium chloride (KCl), 358.15 mg of disodium hydrogen phosphate dodecahydrate ( $\text{Na}_2\text{HPO}_4 \cdot 12\text{H}_2\text{O}$ ), 66.6 mg of calcium chloride ( $\text{CaCl}_2$ ), and 4,236.9 mg of sodium chloride (NaCl). To make a 500 mL solution (pH 7.4), add ultrapure water.

### Animal manipulation

The male mice used in the investigation weighed 13.2 to 20.5 g. After anesthesia, each mouse was secured in a stereotaxic apparatus to expose the skull. After removing the top hair, cotton balls soaked in 75% ethanol were used to disinfect the scalp. The skull surface was cleansed with cotton balls wet with saline until it was plainly visible after the periosteum was gently removed. After exposing the skull, the bregma point was identified and used as the coordinate origin. The target location in the PFC (coordinates: AP: +1.94 mm, ML:  $\pm 0.3$  mm, DV:  $-2.5$  mm) was determined. Precise cranial drilling was performed to create three holes: one for implanting the microdialysis probe guide cannula, and two for anchor screws. The cannula was firmly fixed to the skull using dental cement to ensure stability during normal animal activity. Following cannula implantation, the mice were individually housed under room temperature for a recovery period of 3–5 days. Only those that resumed normal behavior and feeding activity without showing signs of lethargy or other adverse postoperative effects were included in subsequent studies.

### Sample preparation

The mouse was given gas anesthesia on the day of the experiment, and the microdialysis probe was then carefully placed into the guide cannula that had already been implanted. After that, the probe was attached to a microinfusion pump and microdialysis tubing. Microdialysis sampling was started as soon as the mouse regained voluntary mobility when the gas anesthetic was stopped. A microinfusion pump was utilized to perfuse aCSF at a flow rate of  $1.0 \mu\text{l} \cdot \text{min}^{-1}$ . Six dialysate samples were obtained over the course of three hours, with one sample tube being taken every thirty minutes, after a 1.5 h equilibration interval. Immediately after collection, the samples were kept at  $-80^\circ\text{C}$  for UPLC-MS/MS analysis. Upon completion of the experiment, the animal was euthanized via overdose of isoflurane anesthesia combined with cervical dislocation. The brain was rapidly removed, flash-frozen on dry ice, and stored at  $-20^\circ\text{C}$  for subsequent histological verification of probe placement.

### Biological sample preparation

Pipette 25.0  $\mu\text{L}$  of brain microdialysate into a glass UPLC-MS/MS vial. Then, add 25  $\mu\text{l}$  of a  $2 \text{ ng} \cdot \text{ml}^{-1}$  IS working solution to the same vial. Vortex the mixture thoroughly for 10–15 s to ensure complete homogenization. The sample is now ready for UPLC-MS/MS analysis.

### UPLC-MS/MS analysis

An ACQUITY BEH Amide column ( $2.1 \text{ mm} \times 100 \text{ mm}$ ,  $1.7 \mu\text{m}$ ) was used for separation. The mobile phase consisted of (A) 0.2% formic acid in water and (B) acetonitrile. The gradient elution program was set as follows: 0–1 min, 75% B; 1–1.8 min, 65% B; 1.8–2.3 min, 55% B; 2.3–3.2 min, 40% B; 3.2–5.0 min, 40% to 75% B. The flow rate was maintained at  $0.4 \text{ mL/min}$ , and the injection volume was 2  $\mu\text{l}$ . Analysis was performed using an electrospray ionization (ESI) source in positive ion multiple reaction monitoring (MRM) mode. The ion source temperature was set to  $500^\circ\text{C}$ . The curtain gas pressure was 20 psi, the collision gas pressure was 8 kPa, and the ion spray voltage was 5500 V. Both Gas1 and Gas2 were set to 60 psi. Detailed instrument parameters and monitored ion transitions are summarized in (Table 1).

### RT-qPCR

The primer sequences are listed in (Table 2). Total mRNA was extracted from the PFC using the Trizol method, and the concentration and purity of the RNA were measured at 260 nm and 280 nm using an ultra-micro spectrophotometer. The RNA was reverse-transcribed into complementary DNA (cDNA) using a TIANGEN reverse transcription kit under the following reaction conditions:  $42^\circ\text{C}$  for 15 min and  $95^\circ\text{C}$  for 3 min. qPCR was performed using the Real Universal Color Fluorescence Quantitative PreMix (SYBR Green) kit. The RT-PCR amplification conditions consisted of an initial denaturation at  $95^\circ\text{C}$  for 15 min, followed by 40 cycles of  $95^\circ\text{C}$  for 10 s and  $60^\circ\text{C}$  for 25 s. An Illumina RT-PCR system was used for the experiment, and the  $2^{-\Delta\Delta\text{Ct}}$  method

Compound name	Precursor ion(m/z)	Product ion(m/z)	Retention Time(min)	DP(V)	CE(eV)
Glu	148.1	84.2	2.13	45	22
Gly	76.0	30.1	2.06	100	20
GABA	104.2	87.1	1.33	60	15
5-HT	177.2	160.2	1.19	40	17
5-HIAA	192.1	146.2	1.14	100	24
DA	154.2	137.3	1.20	56	14.5
IS	212.0	194.0	1.25	100	20

**Table 1.** Monitoring ion transitions for the seven neurotransmitters are summarized as follows.

Gene	Forward primer	Reverse primer
<i>gria1</i>	GGACAACCTCAAGCGTCCAGA	GTCGGTAGGAATAGCCCACG
<i>gria2</i>	CAGGATTTGGTTTGGTTCCG	CCTTAGTCTGTGTGCGGTGT
<i>gria3</i>	GCAATTCATACAGCGCTGGG	TGCCTCCTCAGGTATCGGAA
<i>gria4</i>	GGCCAGGGAATTGACATGGA	CCTTTCGAGGTCCTGTGCTT
<i>slc6a3</i>	TCACACCTGAGAAAGACCGC	GCAGCTGTCTCCTTCCACTT
<i>slc6a4</i>	CGTCACCTGCTGAGGAGTTT	CCACCTTGCCAGACGTTTGT
<i>slc6a9</i>	CTCTGCCCTGAGCTGTTTCA	GATTTTCTGGGCAGAGGCT
<i>gabra1</i>	CTTGCAACCTGCCTTTGTCC	TTCTTCCGACAGTGTGCTC

**Table 2.** Primer sequences for quantitative real-time polymerase chain reaction.

was used to determine the relative mRNA expression levels of *gria1*, *gria2*, *gria3*, *gria4*, *slc6a3*, *slc6a4*, *slc6a9*, and *gabra1* in the PFC.

### Statistical data analysis

All statistical analyses were performed using GraphPad Prism 9.0 software. Data are presented as the mean  $\pm$  standard error of the mean (SEM). The normality of data within each group was first assessed using the Shapiro–Wilk test. For data conforming to a normal distribution, comparisons between two independent groups were conducted following the pre-specified analytical sequence: (1) TARP  $\gamma$ -8 KO group (vehicle treatment) versus the WT group (vehicle treatment), followed by (2) TARP  $\gamma$ -8 KO group (aniracetam treatment) versus the TARP  $\gamma$ -8 KO group (vehicle treatment). These comparisons were performed using independent-samples *t*-tests. Specifically, the standard unpaired *t*-test was applied when group variances were equal, whereas Welch's corrected *t*-test was applied for comparisons involving unequal variances. For data that violated the normality assumption, the non-parametric Mann–Whitney *U* test was employed for comparisons between two independent groups. Significance levels were defined as follows: \*\*\*\**P* < 0.0001, \*\*\**P* < 0.001, \*\**P* < 0.01, and \**P* < 0.05.

## Results

### Method validation

#### Specificity

Following the standard solution preparation procedure, aCSE, aCSF spiked with mixed standards, and mouse brain microdialysate samples collected 90 min after post-dose perfusion equilibrium were analyzed. The specificity results are shown in (Fig. 1). The results indicate that endogenous components in the processed aCSF do not interfere with the detection of any of the seven analytes. All target compounds demonstrated excellent separation with sharp and symmetrical peak shapes.

#### Linearity and LLOQ

A series of standard working solutions were prepared by diluting the mixed standard stock solution. Using the peak area of the analytes as the y-axis and their concentrations as the x-axis, weighted least squares regression ( $W = 1/X^2$ ) was performed to establish the corresponding regression equations. The limit of detection (LOD) and limit of quantitation (LOQ) were determined at signal-to-noise ratios (S/N) of  $\geq 3$  and  $\geq 10$ , respectively. As shown in (Table 3), all calibration curves exhibited good linearity (correlation coefficient  $R^2 > 0.99$ ), where *y* represents the corrected peak area ratio of the analyte to the internal standard, and *x* denotes the concentration of the analyte. Within their respective linear ranges, the peak areas of all analytes showed satisfactory linear relationships with their concentrations. The lower limits of quantitation (LLOQ) for each analyte in cerebrospinal fluid were as follows: 5.0 ng·mL<sup>-1</sup> for Glu and DA; 50 ng·mL<sup>-1</sup> for Gly; 3 ng·mL<sup>-1</sup> for GABA; 1.5 ng·mL<sup>-1</sup> for 5-HT; and 10 ng·mL<sup>-1</sup> for 5-HIAA.

#### Precision and accuracy

The biological samples with low, medium, and high concentrations of each component were prepared using aCSE, with five parallel preparations for each concentration, followed by injection and analysis. The samples were continuously measured over three days, and the intra-day and inter-day precision and accuracy were calculated by substituting the results into the standard curve equation of the day, as shown in (Table 4). The results demonstrated that the intra-day precision relative standard deviation (RSD) for the three different concentrations was < 8.89%, and the inter-day precision RSD was < 8.9%. The intra-day accuracy Relative Error (RE) absolute value was < 0.85%, and the inter-day accuracy RE absolute value was < 10.7%. These findings indicate that the intra-day and inter-day precision and accuracy for the low, medium, and high concentrations of each neurotransmitter component in the biological samples were satisfactory, and the measurement results of this method all met the acceptable criteria.

#### Stability

Biological samples containing low and high concentrations of each component were prepared using aCSF, with five parallel replicates for each concentration. These samples were stored at 4°C for 8 h and subsequently analyzed, as shown in (Table 5). According to the results, the RSD of the samples ranged from 2.34 to 8.44% after

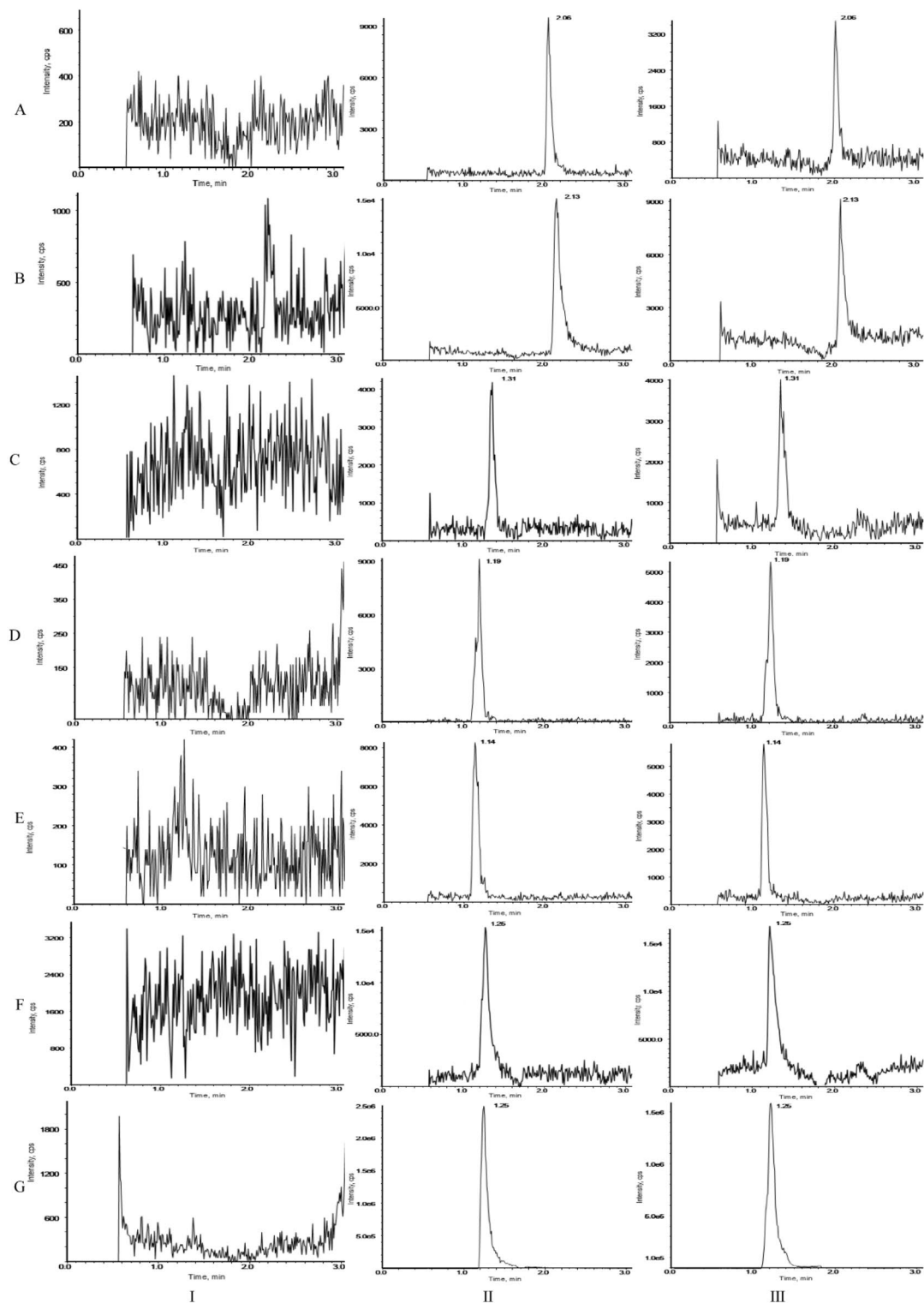


**Fig. 1.** MRM chromatograms of the seven neurotransmitters in brain microdialysate. I. aCSF; II. aCSF spiked with mixed standard solution; III. Brain microdialysate after 90 min perfusion; (A) Gly; (B) Glu; (C) GABA; (D) 5-HT; (E) 5-HIAA; (F) DA; (G) Isoprenaline (IS).

Neurotransmitters	Regression equation	Linear range(ng/mL)	R <sup>2</sup>	LOD(ng/ml)	LOQ (ng/ml)
Glu	Y = 0.000358X + 0.00013	5–245	0.9992	0.5	5.0
Gly	Y = 0.0000105X + 0.000057	50–4900	0.9994	10.0	50.0
GABA	Y = 0.00015X + 0.0000191	3–147	0.9992	0.6	3.0
5-HT	Y = 0.000376X + 9.33 × 10 <sup>-7</sup>	1.5–147	0.9993	0.3	1.5
5-HIAA	Y = 0.0000624X + 0.000609	10–980	0.9996	3.0	10.0
DA	Y = 0.000431X + 3.82 × 10 <sup>-6</sup>	5–245	0.9994	1.0	5.0

**Table 3.** Evaluation of the linearity of the six neurotransmitters.

Analyte	Added(ng/ml)	Intra-day(n = 6)			Inter-day(n = 3)		
		Mean ± SD(ng·mL <sup>-1</sup> )	Precision RSD (%)	Accuracy RE (%)	Mean ± SD(ng·mL <sup>-1</sup> )	Precision RSD (%)	Accuracy RE (%)
Glu	12.5	13.10 ± 1.16	8.89	0.05	12.51 ± 1.11	8.90	0.11
	100	106.00 ± 3.54	3.34	0.06	100.80 ± 5.48	5.43	0.88
	190	197.40 ± 11.87	6.01	0.04	194.60 ± 7.79	4.00	2.46
Gly	150	164.80 ± 8.76	5.31	0.10	159.13 ± 9.49	5.97	6.09
	2000	2248.00 ± 33.47	1.49	0.12	2108.00 ± 116.20	5.51	5.40
	3800	4226.00 ± 88.77	2.10	0.11	4142.67 ± 97.36	2.35	9.02
GABA	7.5	8.26 ± 0.30	3.65	0.10	8.25 ± 0.24	2.95	9.97
	60	66.42 ± 1.33	2.00	0.11	62.97 ± 2.98	4.73	4.96
	114	127.00 ± 2.92	2.30	0.11	126.20 ± 2.51	1.99	10.70
5-HT	4.5	4.77 ± 0.26	5.47	0.06	4.87 ± 0.23	4.71	8.25
	60	66.52 ± 1.39	2.09	0.11	64.27 ± 2.29	3.57	7.12
	114	127.20 ± 3.11	2.45	0.12	125.47 ± 3.23	2.57	10.06
5-HIAA	30	31.84 ± 2.19	6.87	0.06	30.02 ± 2.18	7.25	0.07
	400	413.60 ± 11.19	2.71	-0.46	411.53 ± 8.78	2.13	2.88
	760	738.80 ± 18.14	2.46	0.85	690.93 ± 37.19	5.38	-9.09
DA	12.5	13.16 ± 0.99	7.50	0.05	13.33 ± 0.81	6.11	6.61
	100	111.00 ± 2.35	2.11	0.11	105.56 ± 4.87	4.61	5.56
	190	210.60 ± 4.39	2.09	0.11	208.60 ± 4.32	2.07	9.79

**Table 4.** Precision and accuracy of the six neurotransmitters in brain microdialysate.

Analyte	Added (ng/ml)	8h, 4°C		3 freeze-thaw cycles	
		Precision RSD (%)	Accuracy RE (%)	Precision RSD (%)	Accuracy RE (%)
Glu	12.5	6.09	7.68	6.19	-6.08
	190	3.15	8.53	4.77	0.42
Gly	150	4.11	1.47	4.79	9.07
	3800	2.36	7.11	3.50	3.58
GABA	7.5	4.84	12.13	4.07	12.29
	114	2.34	11.05	2.99	9.65
5-HT	4.5	5.73	12.58	5.90	9.91
	114	2.56	10.00	1.77	-0.88
5-HIAA	30	6.52	7.07	4.70	5.47
	760	3.05	-6.29	6.15	-5.82
DA	12.5	8.44	3.52	10.18	2.24
	190	4.61	7.58	5.91	4.11

**Table 5.** Stability of the six neurotransmitters in brain microdialysate.

8 h of storage at 4 °C, and from 1.77 to 10.18% following three freeze–thaw cycles. The stability test demonstrated that the samples remained stable under the aforementioned conditions.

### Dilution methodology

To validate the reliability of sample dilution at high concentrations, stock solutions of each analyte (Glu, Gly, DA, 5-HT, 5-HIAA, and GABA) were diluted with aCSF at ratios of 1:10 and 1:100. Six replicate samples were prepared for each dilution level. As shown in Table 6, all RSD values were below 15%, indicating that samples exceeding the upper limit of quantitation can still be accurately quantified after tenfold or 100-fold dilution into the linear range of the calibration curve.

Analyte	Dilution factor	Added(ng/ml)	Precision RSD (%)	Accuracy RE (%)
Glu	1:100	20	3.31%	-0.92
	1:10	200	1.77%	-0.83
Gly	1:100	400	3.25%	10.50
	1:10	4000	1.78%	-3.25
GABA	1:100	12	1.89%	-1.53
	1:10	120	1.86%	-4.31
5-HT	1:100	12	3.28%	-7.92
	1:10	120	1.32%	-2.50
5-HIAA	1:100	80	2.64%	-5.21
	1:10	800	1.82%	-6.06
DA	1:100	20	1.76%	-1.08
	1:10	200	0.71%	-0.50

**Table 6.** Dilution integrity of the six neurotransmitters in brain microdialysate.

### Probe recovery

The probe was immersed in a mixed standard solution containing Glu and DA at 200 ng·mL<sup>-1</sup>, GABA and 5-HT at 120 ng·mL<sup>-1</sup>, 5-HIAA at 0.8 µg·mL<sup>-1</sup>, and Gly at 4 µg·mL<sup>-1</sup>. aCSF was perfused at a flow rate of 1 µL·min<sup>-1</sup> to collect the in vitro dialysate. The probe recovery was calculated using the formula  $R = (C_s/C_m) \times 100\%$ , where  $C_m$  represents the concentration of the known mixed standard solution and  $C_s$  denotes the concentration in the microdialysate sample. Based on eight parallel experiments using the in vitro dialysis calculation method, the average recoveries of Glu, Gly, GABA, DA, 5-HT, and 5-HIAA in the PFC were determined to be 18.97, 19.69, 21.08, 12.81, 15.71, and 17.41%, respectively.

### The influence of aniracetam on neurotransmitter levels in dialysate samples from the PFC of TARP $\gamma$ -8 KO mice

The results revealed that, compared with the WT (vehicle) group, TARP  $\gamma$ -8 KO mice exhibited a significant imbalance in neurotransmitter levels (Fig. 2), specifically

Data were confirmed to follow a normal distribution and were analyzed using unpaired *t*-tests. The results showed that Glu levels were significantly higher in TARP  $\gamma$ -8 KO vehicle-treated mice compared to WT (vehicle) group ( $P < 0.0001$ , A). Furthermore, aniracetam treatment significantly reduced Glu levels in the PFC of TARP  $\gamma$ -8 KO mice ( $P < 0.0001$  compared to KO vehicle group, A). Regarding Gly, levels were significantly lower in TARP  $\gamma$ -8 KO (vehicle) mice compared to WT (vehicle) group, while aniracetam treatment significantly increased Gly levels in KO mice. The data were normally distributed, and between-group comparisons were performed using unpaired *t*-tests. Specifically, the comparison between the KO (vehicle) and WT (vehicle) groups was conducted with Welch's correction ( $P < 0.0001$ , B), and the comparison between the KO (aniracetam) and KO vehicle groups was performed using a standard unpaired *t*-test ( $P < 0.0001$ , B). As for GABA, levels were significantly lower in TARP  $\gamma$ -8 KO (vehicle) mice compared to the WT (vehicle) group, while aniracetam administration significantly increased GABA levels. Statistical analysis revealed that the comparison between the KO vehicle and WT vehicle groups was conducted using an unpaired *t*-test with Welch's correction ( $P = 0.0005$ , C), and the comparison between the KO (aniracetam) and KO vehicle groups was performed using a standard unpaired *t*-test ( $P < 0.0001$ , C).

The extracellular levels of monoamine neurotransmitters and a key metabolite were also dysregulated in the KO model and were significantly affected by aniracetam (Fig. 3)

To further investigate the neuromodulatory effects of TARP  $\gamma$ -8 deletion and aniracetam intervention, we measured the extracellular levels of 5-HT, its major metabolite 5-HIAA, and DA in the PFC via in vivo microdialysis. All data met the assumption of normality as assessed by the Shapiro–Wilk test and were analyzed using unpaired *t*-test (with Welch's correction where applicable). Compared with WT (vehicle) group, TARP  $\gamma$ -8 KO (vehicle) mice exhibited a pronounced reduction in PFC 5-HT levels ( $P < 0.0001$ , D). Similarly, the level of 5-HIAA, the primary metabolite of 5-HT, was also significantly lower in KO mice ( $P < 0.0001$ , E). Remarkably, chronic administration of aniracetam effectively reversed these deficits. In TARP  $\gamma$ -8 KO mice, aniracetam treatment significantly elevated both 5-HT ( $P < 0.0001$ , D) and 5-HIAA ( $P < 0.0001$ , E) levels compared to the TARP  $\gamma$ -8 KO (vehicle) group, suggesting a potent modulatory effect of aniracetam on serotonergic neurotransmission in the absence of TARP  $\gamma$ -8. In addition to serotonergic alterations, dopaminergic signaling was also disrupted in KO mice. PFC DA levels were significantly lower in TARP  $\gamma$ -8 KO (vehicle) mice relative to WT (vehicle) ( $P < 0.0001$ , unpaired *t*-test with Welch's correction, F). Importantly, aniracetam treatment partially restored DA levels in KO animals, resulting in a significant increase compared to the TARP  $\gamma$ -8 KO (vehicle) group ( $P < 0.0001$ , unpaired *t*-test with Welch's correction).

Aniracetam alters mRNA expression of key receptors and transporters to explore the molecular mechanisms underlying these neurochemical changes, we analyzed the mRNA expression of related genes in the PFC

As shown in Fig. 4, Compared with the WT (vehicle) group, TARP  $\gamma$ -8 KO (vehicle) mice exhibited significant downregulation in the expression of Glu receptor AMPA subunit genes *gria1* ( $P < 0.05$ ), *gria2* ( $P < 0.01$ ), and *gria3* ( $P < 0.05$ ), while no significant change was observed in *gria4* expression ( $P = 0.0744$ ). Notably, after aniracetam treatment, the expression of *gria1* ( $P < 0.05$ ), *gria2* ( $P < 0.001$ ), and *gria3* ( $P < 0.05$ ) was significantly upregulated

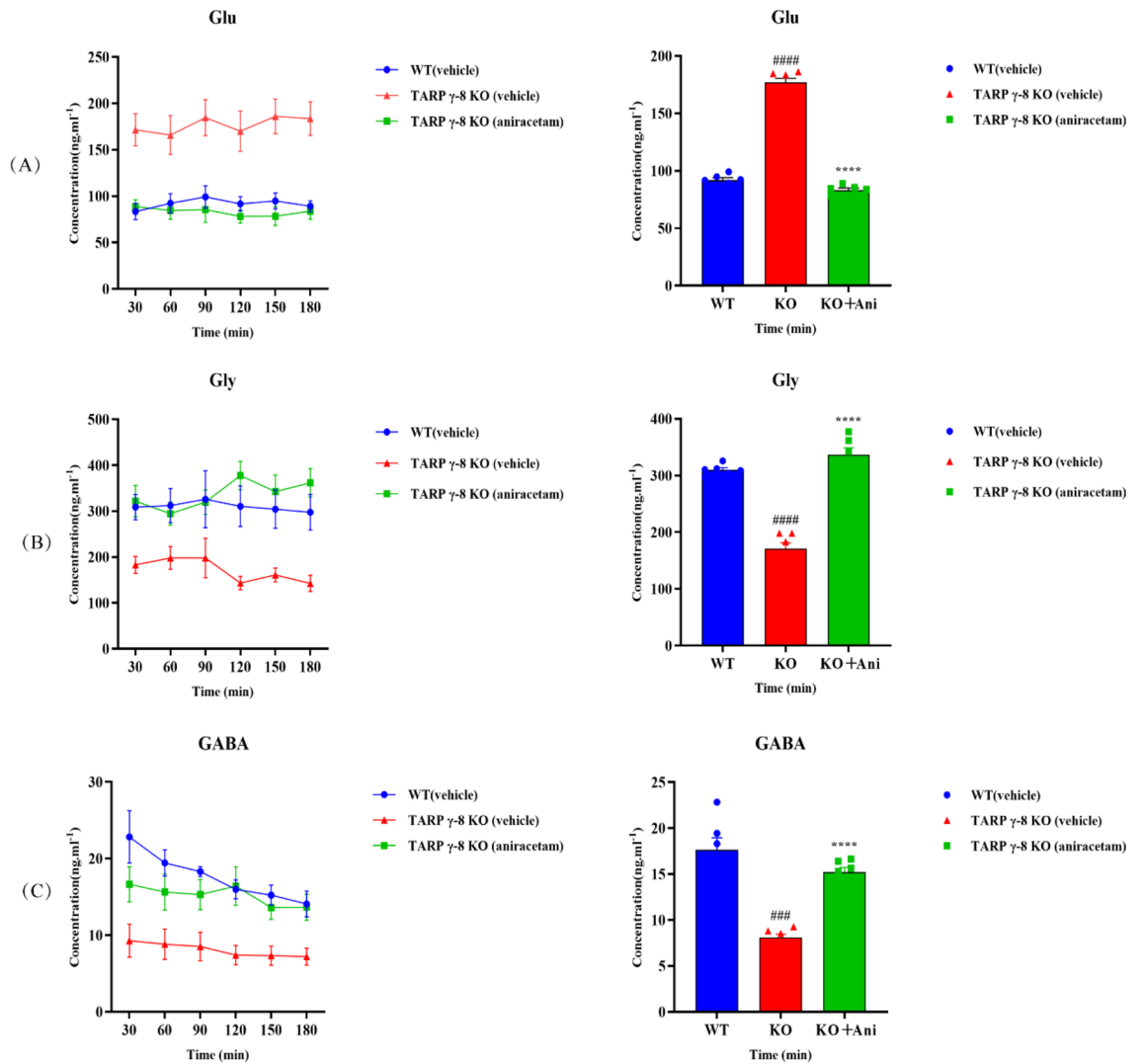


**Fig. 2.** Effects of aniracetam on the levels of Glu, Gly, and GABA in PFC microdialysates of TARP  $\gamma$ -8 KO mice (Mean  $\pm$  SEM,  $n = 8$ ). Microdialysis was used to monitor extracellular neurotransmitter levels. Data are expressed as mean  $\pm$  SEM. **(A)** Glu levels. TARP  $\gamma$ -8 KO (vehicle) mice exhibited significantly higher Glu levels compared to WT (vehicle) mice ( $P < 0.0001$ , unpaired  $t$ -test). Aniracetam treatment significantly lowered Glu levels in KO mice ( $P < 0.0001$ ). **(B)** Gly levels. Gly levels were significantly lower in TARP  $\gamma$ -8 KO (vehicle) mice than in WT (vehicle) ( $P < 0.0001$ , unpaired  $t$ -test with Welch's correction). Aniracetam treatment restored Gly levels in KO mice to a significantly higher level ( $P < 0.0001$ , unpaired  $t$ -test). **(C)** GABA levels. GABA levels were significantly reduced in TARP  $\gamma$ -8 KO (vehicle) mice ( $P < 0.001$ , unpaired  $t$ -test with Welch's correction). Aniracetam administration significantly increased GABA levels in TARP  $\gamma$ -8 KO (vehicle) mice ( $P < 0.0001$ , unpaired  $t$ -test). All data met normality assumption (Shapiro–Wilk test). ####  $P < 0.0001$ , ###  $P < 0.001$ , ##  $P < 0.01$ , #  $P < 0.05$  (TARP  $\gamma$ -8 KO (vehicle) vs. WT (vehicle)); \*\*\*\*  $P < 0.0001$ , \*\*\*  $P < 0.001$ , \*\*  $P < 0.01$ , \*  $P < 0.05$  (TARP  $\gamma$ -8 KO (aniracetam) vs. TARP  $\gamma$ -8 KO (vehicle)).

in TARP  $\gamma$ -8 KO mice, whereas *gria4* expression remained unaffected ( $P = 0.0536$ ). In terms of neurotransmitter transporter genes, the DA transporter *slc6a3* ( $P < 0.001$ ), 5-HT transporter *slc6a4* ( $P < 0.01$ ), and Gly transporter *slc6a9* ( $P < 0.01$ ) were all significantly upregulated in TARP  $\gamma$ -8 KO (vehicle) mice compared to the WT (vehicle) group. Strikingly, aniracetam treatment further reduced the expression levels of these transporter genes in KO mice, with *slc6a3* showing the most significant downregulation ( $P < 0.0001$ ), and *slc6a4* and *slc6a9* also exhibiting significant decreases ( $P < 0.01$  and  $P < 0.01$ , respectively). Regarding the GABAergic system, the expression of the GABA<sub>A</sub> receptor  $\alpha 1$  subunit gene *gabra1* was significantly reduced in TARP  $\gamma$ -8 KO (vehicle) mice ( $P < 0.01$ ). Whereas aniracetam treatment further upregulated its expression levels in KO mice. ( $P < 0.01$ ).

## Discussion

In this study, the regulatory effects of aniracetam, a positive allosteric modulator of AMPARs, on the neurotransmitter network in the PFC of TARP  $\gamma$ -8 KO mice were thoroughly assessed using microdialysis sampling in conjunction with very sensitive UPLC-MS/MS analysis. Our principal finding is that TARP

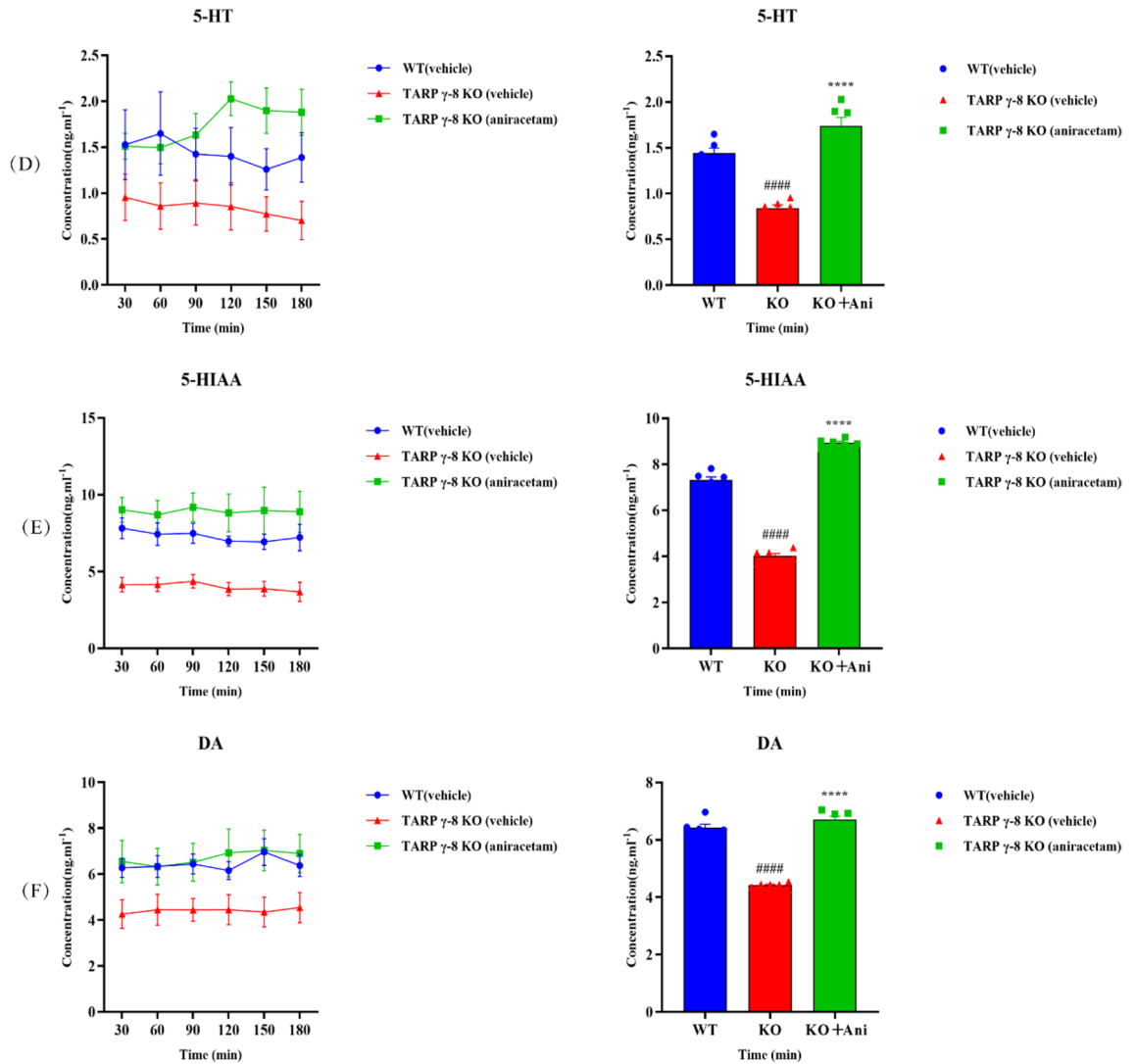


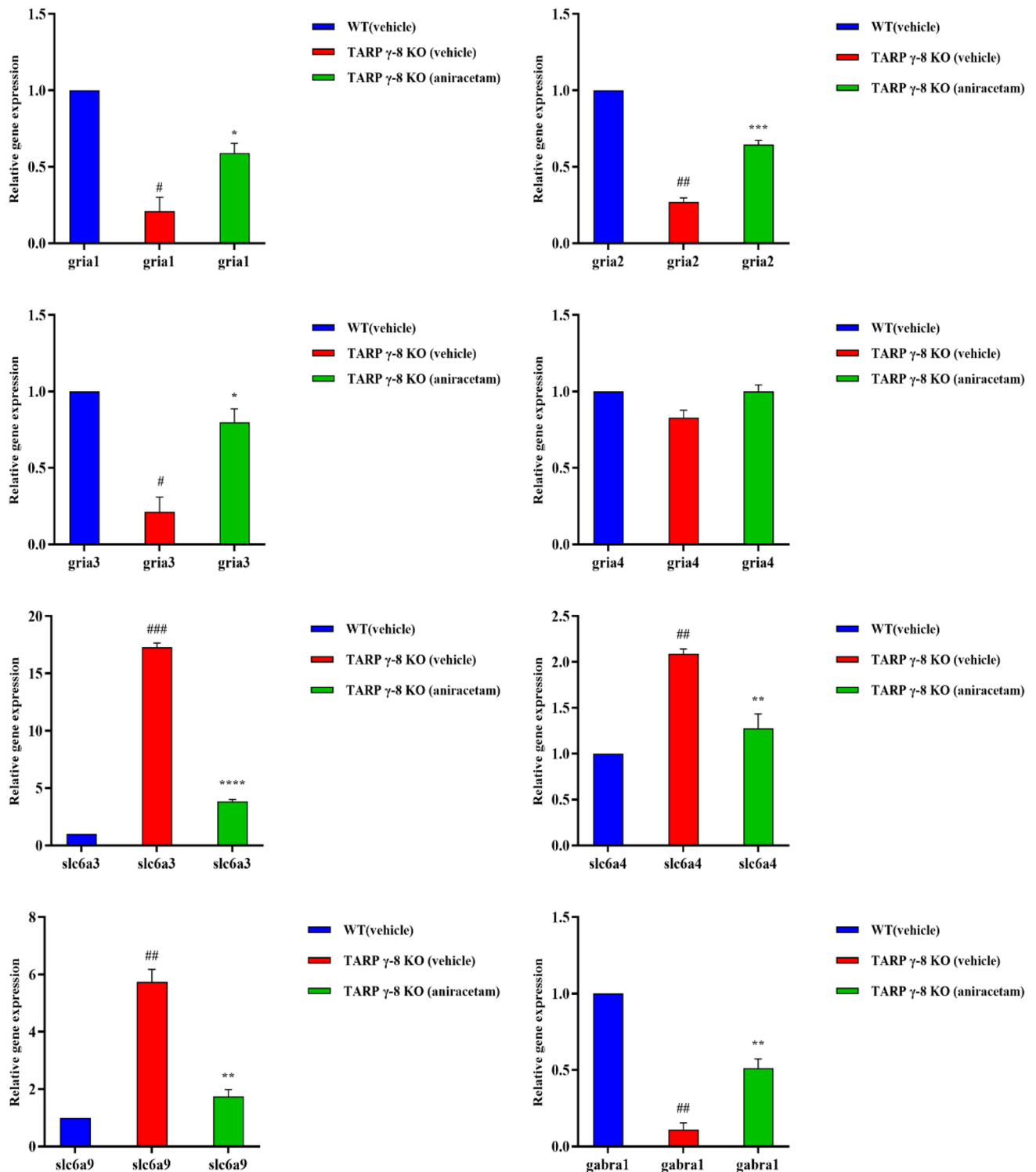
**Fig. 3.** Effects of aniracetam on the Levels of 5-HT, 5-HIAA, and DA in PFC microdialysates of TARP  $\gamma$ -8 KO mice (Mean  $\pm$  SEM,  $n = 8$ ). Microdialysis was used to monitor extracellular neurotransmitter levels. Data are expressed as mean  $\pm$  SEM. **(D)** 5-HT levels. TARP  $\gamma$ -8 KO (vehicle) mice showed significantly lower 5-HT levels compared to WT (vehicle) ( $P < 0.0001$ ). Aniracetam treatment significantly elevated 5-HT levels in KO mice relative to the TARP  $\gamma$ -8 KO (vehicle) group ( $P < 0.0001$ ). **(E)** 5-HIAA levels. 5-HIAA levels were significantly reduced in TARP  $\gamma$ -8 KO (vehicle) mice versus WT (vehicle) ( $P < 0.0001$ ). Aniracetam administration significantly increased 5-HIAA levels in KO mice ( $P < 0.0001$ ). **(F)** DA levels. DA levels were significantly decreased in TARP  $\gamma$ -8 KO (vehicle) mice compared to WT (vehicle) ( $P < 0.0001$ , unpaired  $t$ -test with Welch's correction). Aniracetam treatment significantly restored DA levels in KO mice ( $P < 0.0001$ , unpaired  $t$ -test with Welch's correction). All data met normality assumption and were analyzed by unpaired  $t$ -test (or Welch's correction where specified). ####  $P < 0.0001$ , ###  $P < 0.001$ , ##  $P < 0.01$ , #  $P < 0.05$  (TARP  $\gamma$ -8 KO (vehicle) vs. WT (vehicle)); \*\*\*\*  $P < 0.0001$ , \*\*\*  $P < 0.001$ , \*\*  $P < 0.01$ , \*  $P < 0.05$  (TARP  $\gamma$ -8 KO (aniracetam) vs. TARP  $\gamma$ -8 KO (vehicle)).

$\gamma$ -8 deficiency induces a widespread imbalance in PFC neurotransmission, characterized by glutamatergic hyperexcitability coupled with impaired inhibitory (GABAergic, glycinergic) and monoaminergic (dopaminergic, serotonergic) tone. Aniracetam effectively modulated these abnormalities, demonstrating its multi-target neuromodulatory potential. The underlying mechanisms are examined below from the viewpoints of these two main neurotransmitter systems.

Glu is the most prevalent and extensively used Excitatory Amino Acid (EAA) in the CNS. It is essential for learning, memory, synaptic plasticity, and synaptogenesis. The release of Glu is calcium-dependent: when an action potential reaches the presynaptic terminal, Glu is released into the synaptic cleft, where it binds to corresponding Glu receptors to exert its physiological effects<sup>67</sup>. Glu contributes to the preservation of cellular homeostasis under typical physiological circumstances. Vesicular Glu transporters (VGLUT1 and VGLUT2) in glutamatergic neurons load Glu into synaptic vesicles. When these vesicles depolarize, they fuse with the presynaptic membrane, releasing Glu into the synaptic cleft, where it binds to receptors on the postsynaptic

membrane to complete excitatory synaptic transmission and mediate various physiological processes<sup>68–70</sup>. Bauer et al. found that Glu levels in the anterior cingulate cortex of adult ADHD patients were significantly increased and positively correlated with core symptoms such as hyperactivity and impulsivity<sup>71</sup>. In children with ADHD, methylphenidate treatment significantly reduced Glu levels in related brain regions<sup>72</sup>. Miller et al. further indicated that Glu release was significantly increased in the PFC and striatum of patients with combined-type ADHD, while Glu uptake was abnormal in the PFC but showed no significant difference in the striatum. This suggests the presence of "glutamatergic system hyperactivity" in the PFC of ADHD patients<sup>73</sup>. Our study revealed a significant increase in Glu levels in the microdialysate of the PFC in TARP  $\gamma$ -8 KO mice, which may reflect disrupted synaptic Glu dynamics due to AMPAR dysfunction, potentially involving altered release, reuptake, or metabolic balance. Previous research has demonstrated that TARP  $\gamma$ -8 KO mice exhibit ADHD-like behaviors, including hyperactivity, impulsivity, and cognitive deficits, accompanied by abnormalities in glutamatergic synaptic transmission<sup>49</sup>. This is consistent with our observations, demonstrating that the absence of TARP  $\gamma$ -8 may affect Glu homeostasis by compromising the synaptic stability of AMPARs<sup>74</sup>. Our RT-qPCR results revealed that TARP  $\gamma$ -8 KO mice had downregulated mRNA expression of *gria1-3*, which is consistent with electrophysiological studies showing that TARP  $\gamma$ -8 loss attenuates AMPAR-mediated synaptic transmission and may indicate impairment in AMPAR synthesis or stability<sup>75</sup>. The AMPA receptor positive allosteric modulator aniracetam decreases receptor desensitization and increases channel opening time<sup>56,76</sup>. Our findings show that in TARP  $\gamma$ -8 KO mice, aniracetam administration decreased Glu levels and increased *gria1-3* mRNA expression. These findings imply that aniracetam may work by increasing postsynaptic glutamatergic signaling by improving the transcription or stability of AMPAR subunits. Previous studies have demonstrated that aniracetam slows the desensitization process of AMPARs and prolongs synaptic responses, which is consistent with our observation of up-regulated *gria1-3* mRNA expression<sup>56,76</sup>.

An essential inhibitory neurotransmitter in the CNS is GABA. It plays critical roles in neuronal development and circuit maturation, as well as in maintaining neurotransmitter balance. It is also crucial for promoting sleep, promoting sedation, and controlling anxiety<sup>77</sup>. Studies have indicated that the GABAergic system is particularly vulnerable during abnormal development, as GABAergic neurons originate from a different region of the neural tube compared to glutamatergic neurons, yet they must later integrate functionally<sup>78</sup>. The pathophysiology of ADHD is tightly linked to GABAergic system disruption, according to a large body of experimental and clinical research<sup>41,44,79,80</sup>. Our study observed downregulation of *gabral* expression, which encodes a key subunit mediating fast inhibitory synaptic transmission. Reduced expression of *gabral* may lead to impaired cortical network inhibition, consistent with the behavioral inhibition deficits observed in ADHD patients. Interestingly, there is a particular pattern of correlation between the GABAergic system and the primary symptoms of ADHD. Prior studies have discovered a positive correlation between PFC GABA levels and the ability of people with ADHD to control their impulses<sup>81,82</sup>. The decreased GABA levels observed in the PFC of TARP  $\gamma$ -8 KO mice in our study may contribute to or exacerbate their ADHD-like behaviors, such as hyperactivity and attention deficits. TARP  $\gamma$ -8 serves as an auxiliary subunit of AMPARs and primarily modulates glutamatergic synaptic transmission. However, recent studies have revealed that TARPs, including  $\gamma$ -8, are also expressed in GABAergic neurons and may regulate the synaptic targeting and function of GABA receptors<sup>83</sup>. Therefore, the absence of TARP  $\gamma$ -8 may lead to dysfunction of GABAergic interneurons, thereby reducing GABA synthesis or release. Our study is the first to demonstrate impaired GABAergic system function in TARP  $\gamma$ -8 KO mice, providing new evidence for the Glu-GABA imbalance hypothesis in ADHD. These specific molecular alterations in the GABAergic and glutamatergic synaptic pathways are summarized in (Fig. 5). It has long been believed that aniracetam improves glutamatergic synaptic transmission by altering AMPARs. A direct or indirect regulatory influence on the GABAergic system is suggested by our findings, which also demonstrate a large rise in *gabral* mRNA expression and GABA levels in the PFC. This finding has significant therapeutic implications. The function of aniracetam in regulating the E/I balance is very significant<sup>81,84,85</sup>. By coordinately regulating the glutamatergic and GABAergic systems, aniracetam may potentially facilitate a more comprehensive restoration of brain function. Compared to single-target agents, its multi-target mechanism of action could offer broader therapeutic benefits. As summarized in (Fig. 6), glycinergic neurotransmission was also disrupted in this model. As an essential inhibitory neurotransmitter and a co-agonist of NMDA receptors, Gly regulates inhibitory neurotransmission via Gly receptors while also modulating excitatory signaling through NMDA receptor potentiation. Therefore, maintaining constant Gly levels is critical for keeping normal CNS function<sup>86–88</sup>. Growing evidence suggests that dysregulation of Gly metabolism may be closely linked to the pathological mechanisms of ADHD<sup>89,90</sup>. Glycine transporters (GlyTs) are neurotransmitter transporters that are dependent on sodium and chloride and are in charge of bringing L-glycine into the CNS. As members of the solute carrier family 6 (SLC6), Gly transporters comprise two subtypes: type 1 (*slc6a9*; GlyT1) and type 2 (*slc6a5*; GlyT2). GlyT1 and GlyT2 are both expressed in neurons and astrocytes, but their distribution patterns in the brain are mostly linked to neurotransmission processes. Since GlyT1 is primarily found in astrocytes and is widely distributed throughout the neocortex, thalamus, and hippocampus, where it contributes to glutamatergic neurotransmission, blocking the GlyT1 transporter may alter glutamatergic signaling through NMDA receptors, indicating a possible new therapeutic approach<sup>91–93</sup>. Research on people with ADHD and animal models suggests that impaired inhibitory neurotransmitter function, including that of GABA and Gly, may result in decreased cortical inhibition, which in turn may exacerbate hyperactivity, impulsivity, and attention problems<sup>94,95</sup>. This study is the first to demonstrate reduced Gly levels in the PFC of a TARP  $\gamma$ -8 KO mouse model of ADHD. As an essential inhibitory neurotransmitter and co-agonist of NMDA receptors in the CNS, functional impairment of Gly may disrupt the E/I balance in the cerebral cortex<sup>96</sup>. Notably, Gly modulates synaptic plasticity and cognitive function in the PFC through regulation of NMDA receptor activity<sup>97</sup>, which is closely linked to core ADHD symptoms such as inattention and executive dysfunction. Aniracetam may partially restore NMDA receptor-mediated neuronal plasticity by increasing Gly levels. The major Gly transporter, *slc6a9* (GlyT1), is in charge



of reabsorbing Gly from the synaptic cleft, and the degree of its expression directly affects how well glycinergic neurotransmission works<sup>98</sup>. This study revealed an upregulation of *slc6a9* mRNA expression in TARP  $\gamma$ -8 KO mice, which may contribute to excessive synaptic Gly clearance and exacerbate impairments in inhibitory neurotransmission. Consistent with this finding, clinical studies have reported associations between GlyT1 gene polymorphisms and ADHD susceptibility, suggesting that dysregulated Gly transporter function may represent a potential mechanistic pathway in ADHD<sup>89,99,100</sup>. Aniracetam may potentially upregulate cerebral Gly levels by suppressing *slc6a9* expression and reducing synaptic Gly clearance. This mechanism parallels that of clinically employed Gly reuptake inhibitors, such as SSR504734, which enhance glycinergic neurotransmission through GlyT1 blockade and ameliorate cognitive deficits associated with psychiatric disorders<sup>99</sup>.

DA is one of the most critical neurotransmitters in the PFC and plays a key role in cognitive processes such as attention, executive function, and impulse control. Substantial evidence indicates that dysfunction of the dopaminergic system represents a core pathological mechanism in ADHD<sup>49,101</sup>. One of the most thoroughly

**Fig. 4.** RT-qPCR analysis of mRNA expression of eight Genes in the PFC of TARP  $\gamma$ -8 KO mice (Mean  $\pm$  SEM,  $n = 3$ ). To validate the transcriptomic findings, qPCR was performed to measure the mRNA expression levels of eight genes (*gria1*, *gria2*, *gria3*, *gria4*, *slc6a3*, *slc6a4*, *slc6a9*, and *gabra1*) in the PFC of mice from the WT (vehicle), TARP  $\gamma$ -8 KO (vehicle), and TARP  $\gamma$ -8 (aniracetam) groups. *gria1* expression: TARP  $\gamma$ -8 KO (vehicle) group vs. WT (vehicle) group,  $P < 0.05$ ; TARP  $\gamma$ -8 (aniracetam) group vs. TARP  $\gamma$ -8 KO (vehicle) group,  $P < 0.05$ ; *gria2* expression: TARP  $\gamma$ -8 KO (vehicle) group vs. WT (vehicle) group,  $P < 0.01$ ; TARP  $\gamma$ -8 (aniracetam) group vs. TARP  $\gamma$ -8 KO (vehicle) group,  $P < 0.001$ ; *gria3* expression: TARP  $\gamma$ -8 KO (vehicle) group vs. WT (vehicle) group,  $P < 0.05$ ; TARP  $\gamma$ -8 (aniracetam) group vs. TARP  $\gamma$ -8 KO (vehicle) group,  $P < 0.05$ ; *gria4* expression: TARP  $\gamma$ -8 KO (vehicle) group vs. WT (vehicle) group,  $P = 0.0744$ ; TARP  $\gamma$ -8 (aniracetam) group vs. TARP  $\gamma$ -8 KO (vehicle) group,  $P = 0.0536$ ; *slc6a3* expression: TARP  $\gamma$ -8 KO (vehicle) group vs. WT (vehicle) group,  $P < 0.001$ ; TARP  $\gamma$ -8 (aniracetam) group vs. TARP  $\gamma$ -8 KO (vehicle) group,  $P < 0.0001$ ; *slc6a4* expression: TARP  $\gamma$ -8 KO (vehicle) group vs. WT (vehicle) group,  $P < 0.01$ ; TARP  $\gamma$ -8 (aniracetam) group vs. TARP  $\gamma$ -8 KO (vehicle) group,  $P < 0.01$ ; *slc6a9* expression: TARP  $\gamma$ -8 KO (vehicle) group vs. WT (vehicle) group,  $P < 0.01$ ; TARP  $\gamma$ -8 (aniracetam) group vs. TARP  $\gamma$ -8 KO (vehicle) group,  $P < 0.01$ ; *gabra1* expression: TARP  $\gamma$ -8 KO (vehicle) group vs. WT (vehicle) group,  $P < 0.01$ ; TARP  $\gamma$ -8 (aniracetam) group vs. TARP  $\gamma$ -8 KO (vehicle) group,  $P < 0.01$ . \*\*\*\* $P < 0.0001$ , \*\*\* $P < 0.001$ , \*\* $P < 0.01$ , \* $P < 0.05$  (TARP  $\gamma$ -8 KO (vehicle) vs. WT (vehicle)); \*\*\*\* $P < 0.0001$ , \*\*\* $P < 0.001$ , \*\* $P < 0.01$ , \* $P < 0.05$  (TARP  $\gamma$ -8 KO (aniracetam) vs. TARP  $\gamma$ -8 KO (vehicle)).

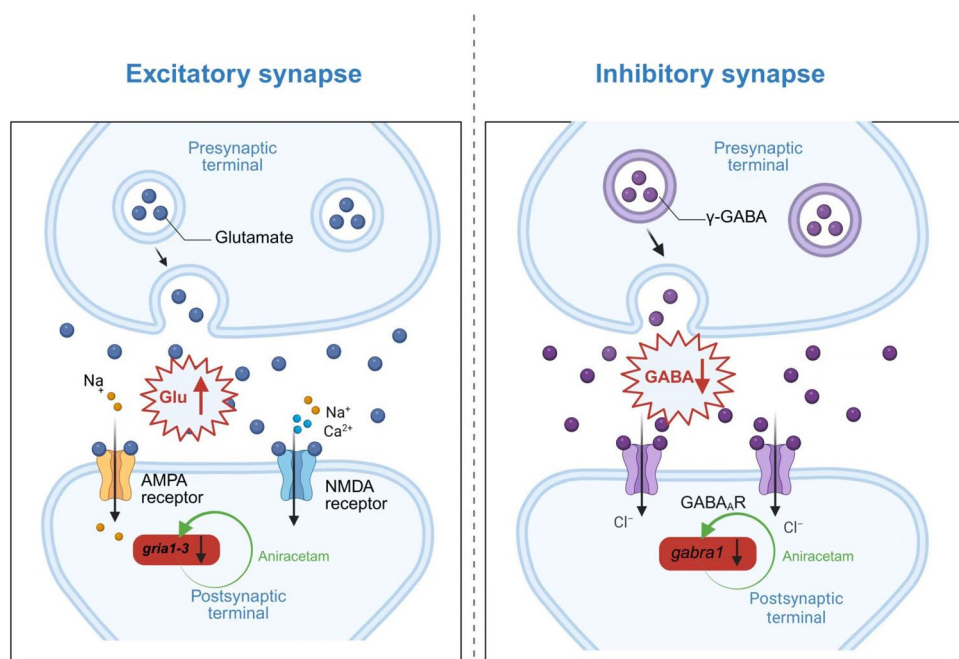


**Fig. 5.** This schematic systematically illustrates the molecular and functional dysregulation mechanisms of the glutamatergic (excitatory) and GABAergic (inhibitory) neurotransmitter systems in the PFC of TARP  $\gamma$ -8 KO mice. Left: Glutamatergic Synaptic Pathway. Molecular Abnormality (red label): The absence of TARP  $\gamma$ -8 protein leads to downregulation ( $\downarrow$ ) of AMPAR subunit genes (*gria1-3*) mRNA expression. Functional Manifestation (explosion-shaped cloud diagram): Glu levels in the synaptic cleft are significantly elevated. Right: GABAergic Synaptic Pathway. Molecular Abnormality (red label): The GABA<sub>A</sub> receptor  $\alpha$ 1 subunit gene (*gabra1*) mRNA expression is downregulated ( $\downarrow$ ). Functional Manifestation (explosion-shaped cloud diagram): Synaptic GABA levels are correspondingly reduced. Intervention Effect (green arrow): Aniracetam treatment reverses the abnormalities in gene expression and neurotransmitter levels described above. Glu, Glutamate; NMDA-R, N-Methyl-d-Aspartate receptor; AMPA-R, Alpha-amino-3-hydroxy-5-methyl-4-isoxazolepropionic acid Receptor; GABA Transporter; GABA<sub>A</sub>, Gamma-Aminobutyric Acid Type A Receptor; *gabra1*, Gamma-Aminobutyric Acid Type A Receptor Alpha 1 Subunit (gene).

studied targets in genetic studies of ADHD is the DAT1 gene, which codes for the synaptic cleft DA reuptake transporter. This focus likely stems from the central role of dopaminergic neurotransmission dysfunction in the pathophysiology of ADHD<sup>102</sup>. The DAT reuptakes DA from the synaptic cleft, hence stopping neurotransmission. By altering the density of DAT at synaptic locations, the amount of active DA accessible for neurotransmission can be directly changed<sup>103</sup>. According to clinical research, people with ADHD have greater DAT density and lower DA levels in the PFC, which causes DA to be cleared from the synaptic cleft too quickly<sup>104</sup>. In this study, TARP  $\gamma$ -8 KO mice had significantly lower levels of DA in the microdialysate of the PFC, a phenomenon that

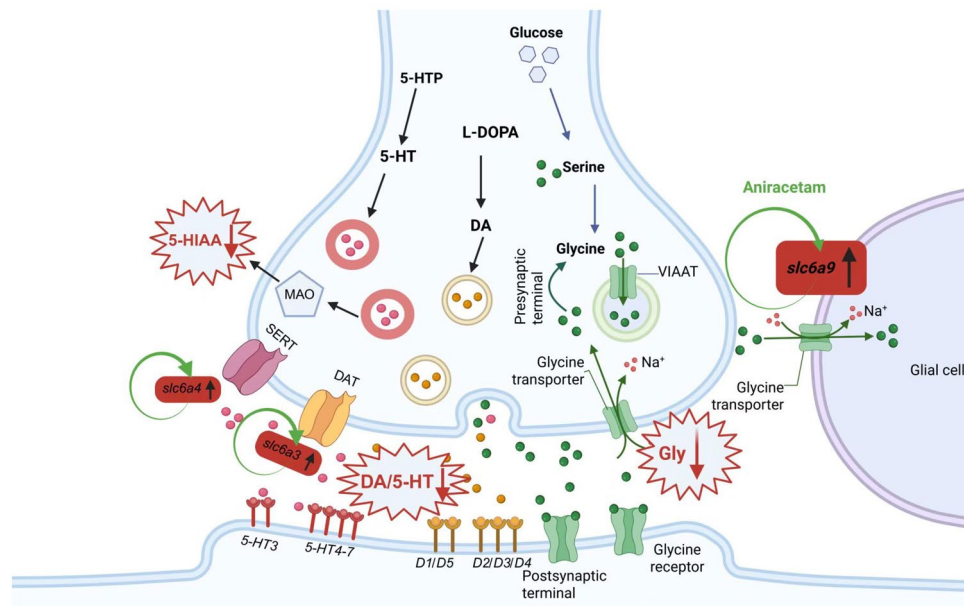


**Fig. 6.** This schematic systematically illustrates the molecular and functional dysregulation mechanisms of the dopaminergic, serotonergic (including its metabolite 5-HIAA), and glycinergic neurotransmitter systems in the PFC of TARP  $\gamma$ -8 KO mice. Dopaminergic System: Molecular Abnormality (red label  $\uparrow$ ): Upregulation of DA transporter gene (*slc6a3*/DAT) expression. Functional manifestation (explosion-shaped cloud diagram): Decreased synaptic DA levels. Serotonergic System: Molecular Abnormality (red label  $\uparrow$ ): Upregulation of 5-HT transporter gene (*slc6a4*/SERT) expression. Functional Manifestation (explosion-shaped cloud diagram): Decreased synaptic 5-HT and its metabolite 5-HIAA levels. Glycinergic system: molecular abnormality (red label  $\uparrow$ ): Upregulation of Gly transporter gene *slc6a9* (GlyT1) mRNA expression. Functional manifestation (explosion-shaped cloud diagram): Decreased synaptic Gly levels. Intervention Effect (green arrow): Aniracetam treatment reverses the abnormalities in gene expression and neurotransmitter levels described above. 5-HT, 5-Hydroxytryptamine, that is, Serotonin; 5-HIAA, 5-Hydroxyindoleacetic Acid; 5-HTP, 5-Hydroxytryptophan; MAO, Monoamine Oxidase; *slc6a4* (SERT), Serotonin Transporter; D1-D5, Subtypes of dopamine receptors; *slc6a3* (DAT), Dopamine Transporter; VIAAT, Vesicular Inhibitory Amino Acid Transporter; *slc6a9*, Solute Carrier Family 6 Member 9 (GlyT1);

was significantly modulated by aniracetam treatment. In addition, RT-qPCR research showed that the PFC of TARP  $\gamma$ -8 KO mice had upregulated DA transporter (*slc6a3*/DAT) mRNA expression, which was markedly downregulated after aniracetam treatment. Increased DAT expression may enhance DA reuptake, leading to reduced extracellular DA levels and upregulation of dopaminergic receptors. These findings align with the functional hypodopaminergic hypothesis of ADHD. Studies by Bai et al. demonstrated that TARP  $\gamma$ -8 KO mice exhibit classic ADHD-like behaviours, including hyperactivity, impulsivity, and cognitive deficits. These behavioural abnormalities are associated with disrupted AMPAR complex function in the hippocampus and impaired regulation of dopaminergic and glutamatergic synaptic transmission in the PFC<sup>49</sup>. Our microdialysis results further confirm that dopaminergic system dysfunction induced by TARP  $\gamma$ -8 deficiency may represent a key neurochemical basis for ADHD-like behaviours. Aniracetam, a nootropic agent, has a mechanism for improving cognitive function that remains incompletely elucidated. This study is the first to show that aniracetam increases extracellular DA levels while downregulating *slc6a3* mRNA expression in the PFC of TARP  $\gamma$ -8 KO mice. This dual effect suggests that aniracetam may modulate dopaminergic neurotransmission through multiple pathways. Aniracetam may prolongs DA activity inside the synaptic cleft and could thereby ameliorate the dopaminergic transmission impairments caused by TARP  $\gamma$ -8 deficiency by decreasing presynaptic DA reuptake by decreasing *slc6a3* expression<sup>49</sup>. This mechanism distinguishes aniracetam from conventional ADHD pharmacotherapies—such as atomoxetine (a selective norepinephrine transporter inhibitor) and methylphenidate (a non-selective dopamine and norepinephrine transporter inhibitor)—underscoring its distinctive mode of action<sup>56,76,105</sup>.

5-HT plays a complex and multifaceted role in various physiological processes, including anxiety, depression, addiction, aggressive behaviour, and impulse control. Given that the core symptoms of ADHD manifest as deficits in inhibitory control and that the disorder is a well-established precursor to various impulse control disorders in adults, researchers hypothesize that the 5-HT system may play a significant role in its pathogenesis. Indeed, accumulating evidence from both human and animal studies indicates that serotonergic neurotransmission is essential for regulating multiple behavioural features of ADHD<sup>106,107</sup>. The inactivation of 5-HT is partially regulated by a reuptake mechanism—upon re-entry into the presynaptic neuron, 5-HT is not metabolically degraded but instead recycled for reuse. This reuptake process is mediated by the serotonin transporter (SERT)<sup>108</sup>. The efficiency of serotonergic neurotransmission is closely linked to the concentration of the neurotransmitter in the synaptic cleft. The primary regulator of synaptic 5-HT levels is the 5-HT transporter,

encoded by the *slc6a4* gene (also known as 5-HTT or SERT), which selectively clears serotonin from the synaptic space. Clinical genetic studies have established associations between *slc6a4* gene polymorphisms and the severity of ADHD symptoms. Specifically, the 5-HTTLPR/rs25531 polymorphism has been linked to more pronounced hyperactive and impulsive symptoms in individuals carrying the S or LG allele<sup>109</sup>. The 5-HTTLPR polymorphism has been extensively studied and is well-established in its association with depression and related disorders, as well as with ADHD<sup>110–113</sup>.

This study revealed significantly reduced levels of 5-HT and 5-HIAA in the cerebrospinal fluid of the PFC in TARP  $\gamma$ -8 KO mice, a finding highly consistent with previous research on the role of TARP  $\gamma$ -8 in neuropsychiatric disorders. As a key brain region for higher cognitive functions, aberrant serotonergic neurotransmission in the PFC may contribute to executive dysfunction—a core symptom of ADHD<sup>111,114–117</sup>. We found that 5-HT and 5-HIAA levels in cerebrospinal fluid significantly increased after aniracetam therapy, indicating that aniracetam may improve serotonergic neurotransmission via a variety of mechanisms. Studies have shown elevated *slc6a4* mRNA expression in TARP  $\gamma$ -8 KO mice, which was reversed by aniracetam administration. *slc6a4* encodes the SERT, a key regulator of synaptic 5-HT concentration and an important target for various psychotropic drugs<sup>109,118</sup>. Our findings indicate that TARP  $\gamma$ -8 deficiency may lead to dysregulation of serotonergic neurotransmission homeostasis, eliciting upregulated *slc6a4* expression as a compensatory response. This observation is highly consistent with recent research on the association between *slc6a4* gene polymorphisms and neuropsychiatric disorders. Multiple studies have demonstrated that specific variants of the *slc6a4* gene, such as the 5-HTTLPR polymorphism, are closely correlated with ADHD symptom severity and therapeutic outcomes<sup>16,119</sup>. This upregulation of *slc6a4* may underlie the observed reduction in extracellular 5-HT, and is consistent with clinical genetic findings linking *slc6a4* polymorphisms to ADHD. In summary, TARP  $\gamma$ -8 deficiency induces broad dysregulation of prefrontal monoaminergic neurotransmission (Fig. 6), which can be reversed by aniracetam treatment.

It is important to note that this study was conducted exclusively in male adolescent mice. While this design helped control for sex-related variables during the initial mechanistic exploration, allowing for a more focused investigation of core mechanisms, the significance of this methodological limitation must be explicitly acknowledged. Accumulating evidence indicates that neurodevelopmental disorders such as ADHD exhibit significant sexual dimorphism across multiple dimensions, including epidemiological characteristics, clinical behavioral phenotypes, related neural circuit functions, and molecular regulatory mechanisms<sup>120–122</sup>. Consequently, conclusions derived from a single-sex (male) animal model should be extrapolated with caution to female individuals or clinical populations. Future research is urgently needed to conduct parallel assessments of aniracetam's behavioral-improving effects and its impact on neurochemical homeostasis in female TARP  $\gamma$ -8 KO mice, and to further explore potential sex-specific regulatory mechanisms. Such studies hold critical scientific and clinical value in systematically elucidating the drug's spectrum of action and enhancing the generalizability and precision of therapeutic strategies. In conclusion, our data support a model wherein aniracetam, initiated by positive modulation of AMPARs, engenders a cascade of modulatory effects across multiple neurotransmitter systems. It appears to modulate the E/I balance in the PFC by enhancing glutamatergic efficiency while simultaneously strengthening GABAergic and glycinergic inhibition, and by boosting monoaminergic neurotransmission. This multi-system synergistic action distinguishes it from conventional single-target ADHD pharmacotherapies<sup>105</sup>.

## Conclusion

This study combined neurochemical assays and molecular biology techniques to investigate the therapeutic mechanisms of aniracetam in a TARP  $\gamma$ -8 KO mouse model of ADHD, yielding comprehensive insights. The results demonstrate that the loss of TARP  $\gamma$ -8 leads to widespread neurotransmitter imbalances and molecular compensatory adaptations in the CNS, characterized by glutamatergic hyperexcitability accompanied by suppressed function in GABAergic, glycinergic, and monoaminergic systems. This overall phenotype closely aligns with the pathophysiological features of ADHD. More importantly, this study provides the first systematic demonstration that aniracetam effectively significantly affects all the aforementioned abnormalities, highlighting its exceptional multi-target neuromodulatory capabilities. The central mechanism can be summarized as follows: through positive allosteric modulation of AMPARs, aniracetam promotes homeostasis in neural circuits. In summary, this study not only validates the TARP  $\gamma$ -8 KO mouse as a highly relevant model for ADHD research, but also provides strong molecular and neurochemical evidence supporting the considerable potential of aniracetam as a multi-target therapeutic agent for ADHD. Our findings provide solid experimental evidence supporting the hypothesis that “AMPA modulation” could serve as a novel therapeutic strategy for ADHD. They also offer robust preclinical data for the potential use of aniracetam in ADHD treatment and deepen our understanding of the role of TARP  $\gamma$ -8 protein in neuropsychiatric disorders. Building upon the current findings, future investigations will encompass a multi-faceted approach to further elucidate the mechanism of aniracetam. First, it will be imperative to systematically evaluate the drug's efficacy and underlying mechanisms in female TARP  $\gamma$ -8 KO mice, allowing for direct comparison with the present male-derived data and thereby enhancing the clinical translatability of the findings. Subsequently, the observed mRNA expression alterations require validation at the protein level through techniques such as Western blot analysis. Finally, employing electrophysiological methodologies will be crucial to directly examine how these molecular changes impact neuronal function, particularly in terms of synaptic plasticity and neural circuit activity. Through the aforementioned multi-layered research strategy, we will provide a more systematic perspective for understanding the underlying mechanisms and lay a more solid theoretical foundation for potential clinical translation.

## Data availability

The datasets used and analyzed during the current study are available from the corresponding author upon reasonable request.

Received: 16 November 2025; Accepted: 30 January 2026

Published online: 05 February 2026

## References

- Berger, I. Diagnosis of attention deficit hyperactivity disorder: much ado about something. *Isr Med. Assoc. J.* **13**, 571–574 (2011).
- Polanczyk, G. V., Salum, G. A., Sugaya, L. S., Caye, A. & Rohde, L. A. Annual research review: A meta-analysis of the worldwide prevalence of mental disorders in children and adolescents. *J. Child Psychol. Psychiatr.* **56**, 345–365 (2015).
- Thomas, R., Sanders, S., Doust, J., Beller, E. & Glasziou, P. Prevalence of attention-deficit/hyperactivity disorder: a systematic review and meta-analysis. *Pediatrics* **135**, e994–e1001 (2015).
- Childress, A. C. & Berry, S. A. Pharmacotherapy of attention-deficit hyperactivity disorder in adolescents. *Drugs* **72**, 309–325 (2012).
- Groman, C. M. J. & Barzman, D. H. The impact of ADHD on morality development. *Atten. Defic. Hyperact. Disord.* **6**, 67–71 (2014).
- Klein, R. G. et al. Clinical and functional outcome of childhood attention-deficit/hyperactivity disorder 33 years later. *Arch. Gen. Psychiatr.* **69**, 1295–1303 (2012).
- Pelham, W. E., Foster, E. M. & Robb, J. A. The economic impact of attention-deficit/hyperactivity disorder in children and adolescents. *J. Pediatr. Psychol.* **32**, 711–727 (2007).
- Sun, H. et al. Psychoradiologic utility of MR imaging for diagnosis of attention deficit hyperactivity disorder: A radiomics analysis. *Radiology* **287**, 620–630 (2018).
- Arnsten, A. F. T. & Pliszka, S. R. Catecholamine influences on prefrontal cortical function: relevance to treatment of attention deficit/hyperactivity disorder and related disorders. *Pharmacol. Biochem. Behav.* **99**, 211–216 (2011).
- Pliszka, S. R. The neuropsychopharmacology of attention-deficit/hyperactivity disorder. *Biol. Psychiatr.* **57**, 1385–1390 (2005).
- Akutagava-Martins, G. C., Salatino-Oliveira, A., Kieling, C. C., Rohde, L. A. & Hutz, M. H. Genetics of attention-deficit/hyperactivity disorder: current findings and future directions. *Expert Rev. Neurother.* **13**, 435–445 (2013).
- Bonvicini, C., Faraone, S. V. & Scassellati, C. Common and specific genes and peripheral biomarkers in children and adults with attention-deficit/hyperactivity disorder. *World J. Biol. Psychiatr.* **19**, 80–100 (2018).
- Gizer, I. R., Ficks, C. & Waldman, I. D. Candidate gene studies of ADHD: a meta-analytic review. *Hum. Genet.* **126**, 51–90 (2009).
- Alsoqih, N. S. et al. A systems biology perspective on childhood ADHD: Neurochemical dysregulation, brain-behavior interactions, and emerging therapeutics. *FASEB J.* **39**, e70981 (2025).
- Gholami, A. & Mortezaee, K. Neurotransmitters in neural circuits and neurological diseases. *ACS Chem. Neurosci.* **16**, 3653–3664 (2025).
- Kessi, M. et al. Attention-deficit/hyperactive disorder updates. *Front. Mol. Neurosci.* **15**, 925049 (2022).
- Pittenger, C., Bloch, M. H. & Williams, K. Glutamate abnormalities in obsessive compulsive disorder: neurobiology, pathophysiology, and treatment. *Pharmacol. Ther.* **132**, 314–332 (2011).
- Nakanishi, S. et al. Glutamate receptors: brain function and signal transduction. *Brain Res. Brain Res. Rev.* **26**, 230–235 (1998).
- Kessels, H. W. & Malinow, R. Synaptic AMPA receptor plasticity and behavior. *Neuron* **61**, 340–350 (2009).
- Traynelis, S. F. et al. Glutamate receptor ion channels: structure, regulation, and function. *Pharmacol. Rev.* **62**, 405–496 (2010).
- Black, M. D. Therapeutic potential of positive AMPA modulators and their relationship to AMPA receptor subunits. A review of preclinical data. *Psychopharmacology* **179**, 154–163 (2005).
- Ward, S. E. & Harries, M. Recent advances in the discovery of selective AMPA receptor positive allosteric modulators. *Curr. Med. Chem.* **17**, 3503–3513 (2010).
- Contreras, D. et al. Methylphenidate restores behavioral and neuroplasticity impairments in the prenatal nicotine exposure mouse model of ADHD: Evidence for involvement of AMPA receptor subunit composition and synaptic spine morphology in the hippocampus. *Int. J. Mol. Sci.* **23**, 7099 (2022).
- Medin, T. et al. Altered  $\alpha$ -amino-3-hydroxy-5-methyl-4-isoxazolepropionic acid (AMPA) receptor function and expression in hippocampus in a rat model of attention-deficit/hyperactivity disorder (ADHD). *Behav. Brain Res.* **360**, 209–215 (2019).
- Hawash, M. et al. Evaluating the neuroprotective potential of novel benzodioxole derivatives in Parkinson's disease via AMPA receptor modulation. *ACS Chem. Neurosci.* **15**, 2334–2349 (2024).
- Qneibi, M. Isoxazole-carboxamide modulators of GluA2-containing  $\alpha$ -amino-3-hydroxy-5-methyl-4-isoxazole-propionic acid receptors in Parkinson's disease. *Chem. Biodivers.* **22**, e202500392 (2025).
- Choquet, D., Opazo, P. & Zhang, H. AMPA receptor diffusional trapping machinery as an early therapeutic target in neurodegenerative and neuropsychiatric disorders. *Transl. Neurodegenerat.* **14**, 8 (2025).
- Kuzuya, A., Ohara, T. & Akamatsu, N. Pathogenesis of comorbid epilepsy in Alzheimer's disease and use of perampanel, an AMPA receptor inhibitor. *Expert Rev. Neurother.* **25**, 1399–1409 (2025).
- Francis, F., Chettri, D. & Nair, D. AMPA receptors in the evolving synapse: structure, function, and disease implications. *Front. Synaptic Neurosci.* **17**, 1661342 (2025).
- Hatano, M. et al. Characterization of patients with major psychiatric disorders with AMPA receptor positron emission tomography. *Mol. Psychiatr.* **30**, 1780–1790 (2025).
- Morrow, J. A., Maclean, J. K. F. & Jamieson, C. Recent advances in positive allosteric modulators of the AMPA receptor. *Curr. Opin. Drug Discov. Devel.* **9**, 571–579 (2006).
- Gross, N. B. & Marshall, J. F. Striatal dopamine and glutamate receptors modulate methamphetamine-induced cortical Fos expression. *Neuroscience* **161**, 1114–1125 (2009).
- Russell, V. A. et al. Response variability in attention-deficit/hyperactivity disorder: a neuronal and glial energetics hypothesis. *Behav. Brain Funct.* **2**, 30 (2006).
- Volkow, N. D. et al. Evidence that methylphenidate enhances the saliency of a mathematical task by increasing dopamine in the human brain. *Am. J. Psychiatr.* **161**, 1173–1180 (2004).
- MacMaster, F. P., Carrey, N., Sparkes, S. & Kusumakar, V. Proton spectroscopy in medication-free pediatric attention-deficit/hyperactivity disorder. *Biol. Psychiatr.* **53**, 184–187 (2003).
- Pavic, A., Holmes, A. O. M., Postis, V. L. G. & Goldman, A. Glutamate transporters: a broad review of the most recent archaeal and human structures. *Biochem. Soc. Trans.* **47**, 1197–1207 (2019).
- Keunen, K., van Elburg, R. M., van Bel, F. & Benders, M. J. N. L. Impact of nutrition on brain development and its neuroprotective implications following preterm birth. *Pediatr Res.* **77**, 148–155 (2015).
- Wu, C. & Sun, D. GABA receptors in brain development, function, and injury. *Metab. Brain Dis.* **30**, 367–379 (2015).
- Chesselet, M., Plotkin, J. L., Wu, N. & Levine, M. S. Development of striatal fast-spiking GABAergic interneurons. *Prog. Brain Res.* **160**, 261–272 (2007).

40. Jahanshahi, M., Obeso, I., Rothwell, J. C. & Obeso, J. A. A fronto-striato-subthalamic-pallidal network for goal-directed and habitual inhibition. *Nat. Rev. Neurosci.* **16**, 719–732 (2015).
41. Ferranti, A. S., Luessen, D. J. & Niswender, C. M. Novel pharmacological targets for GABAergic dysfunction in ADHD. *Neuropharmacology* **249**, 109897 (2024).
42. Mamiya, P. C. et al. Reduced Glx and GABA Inductions in the anterior cingulate cortex and caudate nucleus are related to impaired control of attention in attention-deficit/hyperactivity disorder. *Int. J. Mol. Sci.* **23**, 4677 (2022).
43. Pang, E. W. et al. Cerebellar gamma-aminobutyric acid: Investigation of group effects in neurodevelopmental disorders. *Autism Res.: Off. J. Int. Soc. Autism Res.* **16**, 535–542 (2023).
44. Edden, R. A. E., Crocetti, D., Zhu, H., Gilbert, D. L. & Mostofsky, S. H. Reduced GABA concentration in attention-deficit/hyperactivity disorder. *Arch. Gen. Psychiatr.* **69**, 750–753 (2012).
45. Faraone, S. V. et al. Attention-deficit/hyperactivity disorder. *Nat. Rev. Dis. Primers* **1**, 15020 (2015).
46. Thapar, A. & Cooper, M. Attention deficit hyperactivity disorder. *Lancet* **387**, 1240–1250 (2016).
47. Li, Y. et al. Deficiency of tumor suppressor NDRG2 leads to attention deficit and hyperactive behavior. *J. Clin. Invest.* **127**, 4270–4284 (2017).
48. Won, H. et al. GIT1 is associated with ADHD in humans and ADHD-like behaviors in mice. *Nat. Med.* **17**, 566–572 (2011).
49. Bai, W. et al. Deficiency of transmembrane AMPA receptor regulatory protein  $\gamma$ -8 leads to attention-deficit hyperactivity disorder-like behavior in mice. *Zool. Res.* **43**, 851–870 (2022).
50. Demontis, D. et al. Genome-wide analyses of ADHD identify 27 risk loci, refine the genetic architecture and implicate several cognitive domains. *Nat. Genet.* **55**, 198–208 (2023).
51. Cheng, J., Liu, A., Shi, M. Y. & Yan, Z. Disrupted glutamatergic transmission in prefrontal cortex contributes to behavioral abnormality in an animal model of ADHD. *Neuropsychopharmacol.: Off. Public. Am. College Neuropsychopharmacol.* **42**, 2096–2104 (2017).
52. Alibrandi, S. et al. Multifaceted disruption of AMPA receptor signaling by CACNG8 variants: Integrated evidence from human genetics and molecular simulation. *Comput. Struct. Biotechnol. J.* **27**, 4257–4281 (2025).
53. Peng, S. et al. SNP rs10420324 in the AMPA receptor auxiliary subunit TARP  $\gamma$ -8 regulates the susceptibility to antisocial personality disorder. *Sci. Rep.* **11**, 11997 (2021).
54. Wijayawardhane, N. et al. Postnatal aniracetam treatment improves prenatal ethanol induced attenuation of AMPA receptor-mediated synaptic transmission. *Neurobiol. Dis.* **26**, 696–706 (2007).
55. Elston, T. W. et al. Aniracetam does not alter cognitive and affective behavior in adult C57BL/6J mice. *PLoS ONE* **9**, e104443 (2014).
56. Jin, R. et al. Mechanism of positive allosteric modulators acting on AMPA receptors. *J. Neurosci.* **25**, 9027–9036 (2005).
57. Vaglenova, J. et al. Aniracetam reversed learning and memory deficits following prenatal ethanol exposure by modulating functions of synaptic AMPA receptors. *Neuropsychopharmacology* **33**, 1071–1083 (2008).
58. Love, R. W. B. Aniracetam: An evidence-based model for preventing the accumulation of amyloid- $\beta$  plaques in Alzheimer's disease. *J. Alzheimer's Dis.: JAD* **98**, 1235–1241 (2024).
59. Yuan, X., Gao, L., Peng, Y., She, T. & Wang, J. A deep representation learning algorithm on drug-target interaction to screen novel drug candidates for Alzheimer's disease. *Artif. Intell. Med.* **171**, 103301 (2026).
60. Endo, H. et al. Pharmacokinetic study of aniracetam in elderly patients with cerebrovascular disease. *Behav. Brain Res.* **83**, 243–244 (1997).
61. Katsunuma, H. et al. Treatment of insomnia by concomitant therapy with zopiclone and aniracetam in patients with cerebral infarction, cerebroatrophy, Alzheimer's disease and Parkinson's disease. *Psychiatr. Clin. Neurosci.* **52**, 198–200 (1998).
62. Malykh, A. G. & Sadaia, M. R. Piracetam and piracetam-like drugs: from basic science to novel clinical applications to CNS disorders. *Drugs* **70**, 287–312 (2010).
63. Baranova, A. I., Whiting, M. D. & Hamm, R. J. Delayed, post-injury treatment with aniracetam improves cognitive performance after traumatic brain injury in rats. *J. Neurotrauma* **23**, 1233–1240 (2006).
64. Martin, J. R., Moreau, J. L. & Jenck, F. Aniracetam reverses memory impairment in rats. *Pharmacol. Res.* **31**, 133–136 (1995).
65. Phillips, H., McDowell, A., Mielby, B. S., Tucker, I. G. & Colombo, M. Aniracetam does not improve working memory in neurologically healthy pigeons. *PLoS ONE* **14**, e0215612 (2019).
66. Sun, X., Cui, J., Bai, H., Zhang, W. & Bai, W. Aniracetam ameliorates attention deficit hyperactivity disorder behavior in adolescent mice. *eNeuro* **12**, 524–578 (2025).
67. Lee, Y., Gaskins, D., Anand, A. & Shekhar, A. Glia mechanisms in mood regulation: a novel model of mood disorders. *Psychopharmacology* **191**, 55–65 (2007).
68. Li, X., Wang, W., Yan, J. & Zeng, F. Glutamic acid transporters: targets for neuroprotective therapies in Parkinson's disease. *Front. Neurosci.* **15**, 678154 (2021).
69. Omote, H., Miyaji, T., Juge, N. & Moriyama, Y. Vesicular neurotransmitter transporter: bioenergetics and regulation of glutamate transport. *Biochemistry* **50**, 5558–5565 (2011).
70. Shigeri, Y., Seal, R. P. & Shimamoto, K. Molecular pharmacology of glutamate transporters, EAATs and VGLUTs. *Brain Res. Brain Res. Rev.* **45**, 250–265 (2004).
71. Bauer, J. et al. Hyperactivity and impulsivity in adult attention-deficit/hyperactivity disorder is related to glutamatergic dysfunction in the anterior cingulate cortex. *World J. Biol. Psychiatr.: Off. J. World Federat. Soc. Biol. Psychiatr.* **19**, 538–546 (2018).
72. Wiguna, T., Guerrero, A. P. S., Wibisono, S. & Sastroasmoro, S. The Amygdala's neurochemical ratios after 12 weeks administration of 20 mg Long-acting methylphenidate in children with attention deficit and hyperactivity disorder: A pilot study using (1) H magnetic resonance spectroscopy. *Clin. Psychopharmacol. Neurosci.: Off. Sci. J. Korean College Neuropsychopharmacol.* **12**, 137–141 (2014).
73. Miller, E. M., Pomerleau, F., Huettl, P., Gerhardt, G. A. & Glaser, P. E. A. Aberrant glutamate signaling in the prefrontal cortex and striatum of the spontaneously hypertensive rat model of attention-deficit/hyperactivity disorder. *Psychopharmacology* **231**, 3019–3029 (2014).
74. Cho, C., St-Gelais, F., Zhang, W., Tomita, S. & Howe, J. R. Two families of TARP isoforms that have distinct effects on the kinetic properties of AMPA receptors and synaptic currents. *Neuron* **55**, 890–904 (2007).
75. Yu, J. et al. Hippocampal AMPA receptor assemblies and mechanism of allosteric inhibition. *Nature* **594**, 448–453 (2021).
76. Ito, I., Tanabe, S., Kohda, A. & Sugiyama, H. Allosteric potentiation of quisqualate receptors by a nootropic drug aniracetam. *J. Physiol.* **424**, 533–543 (1990).
77. Rowley, N. M., Madsen, K. K., Schousboe, A. & Steve White, H. Glutamate and GABA synthesis, release, transport and metabolism as targets for seizure control. *Neurochem. Int.* **61**, 546–558 (2012).
78. Anderson, S. A. et al. Mutations of the homeobox genes Dlx-1 and Dlx-2 disrupt the striatal subventricular zone and differentiation of late born striatal neurons. *Neuron* **19**, 27–37 (1997).
79. Ende, G. et al. Impulsivity and aggression in female BPD and ADHD patients: Association with ACC glutamate and GABA concentrations. *Neuropsychopharmacol.: Off. Public. Am. College Neuropsychopharmacol.* **41**, 410–418 (2016).
80. Kim, Y. S., Woo, J., Lee, C. J. & Yoon, B. Decreased glial GABA and tonic inhibition in cerebellum of mouse model for attention-deficit/hyperactivity disorder (ADHD). *Exp. Neurobiol.* **26**, 206–212 (2017).
81. Bollmann, S. et al. Developmental changes in gamma-aminobutyric acid levels in attention-deficit/hyperactivity disorder. *Transl. Psychiatr.* **5**, e589 (2015).

82. Boy, F. et al. Individual differences in subconscious motor control predicted by GABA concentration in SMA. *Curr. Biol.* **20**, 1779–1785 (2010).
83. Tomita, S. et al. Functional studies and distribution define a family of transmembrane AMPA receptor regulatory proteins. *J. Cell Biol.* **161**, 805–816 (2003).
84. Hai, T. et al. Magnetic resonance spectroscopy of gamma-aminobutyric acid and glutamate concentrations in children with attention-deficit/hyperactivity disorder. *JAMA Netw. Open* **3**, e2020973 (2020).
85. Naaijen, J. et al. Glutamatergic and GABAergic gene sets in attention-deficit/hyperactivity disorder: association to overlapping traits in ADHD and autism. *Transl. Psychiatr.* **7**, e999 (2017).
86. Kemp, J. A. & Leeson, P. D. The glycine site of the NMDA receptor—five years on. *Trends Pharmacol. Sci.* **14**, 20–25 (1993).
87. Lynch, G. AMPA receptor modulators as cognitive enhancers. *Curr. Opin. Pharmacol.* **4**, 4–11 (2004).
88. Sohal, V. S. & Rubenstein, J. L. R. Excitation-inhibition balance as a framework for investigating mechanisms in neuropsychiatric disorders. *Mol. Psychiatr.* **24**, 1248–1257 (2019).
89. Chang, J. P., Lane, H. & Tsai, G. E. Attention deficit hyperactivity disorder and N-methyl-D-aspartate (NMDA) dysregulation. *Curr. Pharm. Des.* **20**, 5180–5185 (2014).
90. Kristensen, A. S. et al. SLC6 neurotransmitter transporters: structure, function, and regulation. *Pharmacol. Rev.* **63**, 585–640 (2011).
91. Lopez-Corcuera, B. et al. Differential properties of two stably expressed brain-specific glycine transporters. *J. Neurochem.* **71**, 2211–2219 (1998).
92. Marques, B. L. et al. Neurobiology of glycine transporters: From molecules to behavior. *Neurosci. Biobehav. Rev.* **118**, 97–110 (2020).
93. Smith, K. E. et al. Cloning and expression of a high affinity taurine transporter from rat brain. *Mol. Pharmacol.* **42**, 563–569 (1992).
94. He, B. et al. A cross-sectional survey of preschool children: Exploring heavy metal exposure, neurotransmitters, and neurobehavioural relationships and mediation effects. *Ecotoxicol. Environ. Saf.* **220**, 112391 (2021).
95. Ye, J. et al. Presynaptic glycine receptors on GABAergic terminals facilitate discharge of dopaminergic neurons in ventral tegmental area. *J. Neurosci.* **24**, 8961–8974 (2004).
96. D'Souza, D. C. et al. Glycine transporter inhibitor attenuates the psychotomimetic effects of ketamine in healthy males: preliminary evidence. *Neuropsychopharmacology* **37**, 1036–1046 (2012).
97. Bergeron, R., Meyer, T. M., Coyle, J. T. & Greene, R. W. Modulation of N-methyl-D-aspartate receptor function by glycine transport. *Proc. Natl. Acad. Sci. USA* **95**, 15730–15734 (1998).
98. Eulenburg, V., Armsen, W., Betz, H. & Gomez, J. Glycine transporters: essential regulators of neurotransmission. *Trends Biochem. Sci.* **30**, 325–333 (2005).
99. Depoortere, R. et al. Neurochemical, electrophysiological and pharmacological profiles of the selective inhibitor of the glycine transporter-1 SSR504734, a potential new type of antipsychotic. *Neuropsychopharmacology* **30**, 1963–1985 (2005).
100. Shikanai, H. Advances in the pathophysiology and drug discovery of novel therapeutics for attention-deficit/hyperactivity disorder. *Yakugaku Zasshi* **144**, 1039–1044 (2024).
101. Tripp, G. & Wickens, J. Using rodent data to elucidate dopaminergic mechanisms of ADHD: Implications for human personality. *Personal. Neurosci.* **7**, e2 (2024).
102. Bacanlı, A. et al. Effects of the dopamine transporter gene on neuroimaging findings in different attention deficit hyperactivity disorder presentations. *Brain Imaging Behav.* **15**, 1103–1114 (2021).
103. Waldie, K. E. et al. Dopamine transporter (DAT1/SLC6A3) polymorphism and the association between being born small for gestational age and symptoms of ADHD. *Behav. Brain Res.* **333**, 90–97 (2017).
104. Madras, B. K., Miller, G. M. & Fischman, A. J. The dopamine transporter and attention-deficit/hyperactivity disorder. *Biol. Psychiatr.* **57**, 1397–1409 (2005).
105. Mechler, K., Banaschewski, T., Hohmann, S. & Hage, A. Evidence-based pharmacological treatment options for ADHD in children and adolescents. *Pharmacol. Ther.* **230**, 107940 (2022).
106. New, A. S. et al. Suicide, impulsive aggression, and HTR1B genotype. *Biol. Psychiatr.* **50**, 62–65 (2001).
107. Quist, J. F. & Kennedy, J. L. Genetics of childhood disorders: XXIII. ADHD, Part 7: The serotonin system. *J. Am. Acad. Child Adolesc. Psychiatr.* **40**, 253–256 (2001).
108. Sur, C., Betz, H. & Schloss, P. Immunocytochemical detection of the serotonin transporter in rat brain. *Neuroscience* **73**, 217–231 (1996).
109. Gadow, K. D. et al. Allele-specific associations of 5-HTTLPR/rs25531 with ADHD and autism spectrum disorder. *Prog. Neuropsychopharmacol. Biol. Psychiatr.* **40**, 292–297 (2013).
110. Heiser, P. et al. Family-based association study of serotonergic candidate genes and attention-deficit/hyperactivity disorder in a German sample. *J. Neural Transm. (Vienna)* **114**, 513–521 (2007).
111. Jackson, E. F., Riley, T. B. & Overton, P. G. Serotonin dysfunction in ADHD. *J. Neurodev. Disord.* **17**, 20 (2025).
112. Lotrich, F. E. & Pollock, B. G. Meta-analysis of serotonin transporter polymorphisms and affective disorders. *Psychiatr. Genet.* **14**, 121–129 (2004).
113. Manor, I. et al. Family-based association study of the serotonin transporter promoter region polymorphism (5-HTTLPR) in attention deficit hyperactivity disorder. *Am. J. Med. Genet.* **105**, 91–95 (2001).
114. Da Cunha-Bang, S. et al. The association between brain serotonin transporter binding and impulsivity and aggression in healthy individuals. *J. Psychiatr. Res.* **165**, 1–6 (2023).
115. Oades, R. D. et al. The influence of serotonin- and other genes on impulsive behavioral aggression and cognitive impulsivity in children with attention-deficit/hyperactivity disorder (ADHD): Findings from a family-based association test (FBAT) analysis. *Behav. Brain Funct.* **4**, 48 (2008).
116. Weinberg-Wolf, H. et al. The effects of 5-hydroxytryptophan on attention and central serotonin neurochemistry in the rhesus macaque. *Neuropsychopharmacology* **43**, 1589–1598 (2018).
117. Wingen, M., Kuypers, K. P. C., van de Ven, V., Formisano, E. & Ramaekers, J. G. Sustained attention and serotonin: a pharmacofMRI study. *Hum. Psychopharmacol.* **23**, 221–230 (2008).
118. Wang, T., Shi, L., Luo, Q., Wang, Y. & Zhao, H. SLC6 transporters as pharmacological targets in depression: Molecular mechanisms and therapeutic strategies. *Biochem. Pharmacol.* **242**, 117210 (2025).
119. Hanna, S. et al. The interplay between SLC6A4 and HTR1A genetic variants that may lead to antidepressant failure. *Pharmacogenom. J.* **25**, 13 (2025).
120. Müller, E. D. & Fender, A. C., Sex differences in the response to treatment of attention deficit hyperactivity disorder. *Naunyn-Schmiedeberg's Arch. Pharmacol.* 10–1007 (2025).
121. Rucklidge, J. J. Gender differences in attention-deficit/hyperactivity disorder. *Psychiatr. Clin. North Am.* **33**, 357–373 (2010).
122. Willcutt, E. G. The prevalence of DSM-IV attention-deficit/hyperactivity disorder: a meta-analytic review. *Neurotherapeut.: J. Am. Soc. Exp. Neurotherapeut.* **9**, 490–499 (2012).

## Author contributions

J.C. conceived and designed the study. X.S. developed the methodology. W.B. conducted the formal analysis and

developed software. W.Z. performed validation. X.S., J.C., and S.S. conducted the investigation. W.Z. and W.B. curated the data. H.B. wrote the original draft. X.S. and J.C. reviewed and edited the manuscript. S.S. created visualizations. W.Z. supervised the project. W.B. administered the project. All authors have read and agreed to the published version of the manuscript.

### Funding

The authors declare that financial support was received for the research and publication of this article. This study was funded by the Hebei Provincial Government-funded Clinical Medicine Outstanding Talents Program.

### Declarations

### Competing interests

The authors declare no competing interests.

### Institutional review board statement

This study was approved by the Animal Ethics Committee of the General Hospital of Hebei (Approval No.: 2024-DW-038, Shijiazhuang, China). All experimental procedures were conducted in accordance with the ethical guidelines and regulations for animal welfare established by the General Hospital of Hebei and followed the recommendations of the ARRIVE guidelines for reporting in vivo experiments.

### Additional information

**Correspondence** and requests for materials should be addressed to W.Z. or W.-J.B.

**Reprints and permissions information** is available at [www.nature.com/reprints](http://www.nature.com/reprints).

**Publisher's note** Springer Nature remains neutral with regard to jurisdictional claims in published maps and institutional affiliations.

**Open Access** This article is licensed under a Creative Commons Attribution-NonCommercial-NoDerivatives 4.0 International License, which permits any non-commercial use, sharing, distribution and reproduction in any medium or format, as long as you give appropriate credit to the original author(s) and the source, provide a link to the Creative Commons licence, and indicate if you modified the licensed material. You do not have permission under this licence to share adapted material derived from this article or parts of it. The images or other third party material in this article are included in the article's Creative Commons licence, unless indicated otherwise in a credit line to the material. If material is not included in the article's Creative Commons licence and your intended use is not permitted by statutory regulation or exceeds the permitted use, you will need to obtain permission directly from the copyright holder. To view a copy of this licence, visit <http://creativecommons.org/licenses/by-nc-nd/4.0/>.

© The Author(s) 2026